

# Combining Optimal Transport and Embedding-Based Approaches for More Expressiveness in Unsupervised Graph Alignment

Songyang Chen

Yu Liu<sup>†</sup>

Beijing Jiaotong University  
{songyangchen,yul}@bjtu.edu.cn

Zexuan Wang

Youfang Lin

Beijing Jiaotong University  
{zexuanwang,yflin}@bjtu.edu.cn

Lei Zou

Peking University  
{zoulei}@pku.edu.cn

Yuxing Chen

Anqun Pan

Tencent Inc.  
{axingguchen,aaronpan}@tencent.com

## ABSTRACT

Unsupervised graph alignment finds the one-to-one node correspondence between a pair of attributed graphs by only exploiting graph structure and node features. One category of existing works first computes the node representation and then matches nodes with close embeddings, which is intuitive but lacks a clear objective tailored for graph alignment in the unsupervised setting. The other category reduces the problem to optimal transport (OT) via Gromov-Wasserstein (GW) learning with a well-defined objective but leaves a large room for exploring the design of transport cost. We propose a principled approach to combine their advantages motivated by theoretical analysis of model expressiveness. By noticing the limitation of discriminative power in separating matched and unmatched node pairs, we improve the cost design of GW learning with feature transformation, which enables feature interaction across dimensions. Besides, we propose a simple yet effective embedding-based heuristic inspired by the Weisfeiler-Lehman test and add its prior knowledge to OT for more expressiveness when handling non-Euclidean data. Moreover, we are the first to guarantee the one-to-one matching constraint by reducing the problem to maximum weight matching. The algorithm design effectively combines our OT and embedding-based predictions via stacking, an ensemble learning strategy. We propose a model framework named CombAlign integrating all the above modules to refine node alignment progressively. Through extensive experiments, we demonstrate significant improvements in alignment accuracy compared to state-of-the-art approaches and validate the effectiveness of the proposed modules.

## 1 INTRODUCTION

The unsupervised graph alignment problem predicts the node correspondence between two attributed graphs given their topological structure and node features as inputs. It has a wide range of applications such as linking the same identity across different social networks (e.g., Facebook and Weibo) [21, 44, 63], matching scholar accounts between multiple academic platforms (e.g., ACM and DBLP) [43, 67], various computer vision tasks including image alignment [2] and shape model learning [13], as well as the approximate computation of graph edit distance [23, 33]. Since the nodes to be aligned do not necessarily have identical graph structure and

node features, which is referred to as the *structure and feature inconsistency* [44], the problem remains a challenge, especially in the *unsupervised* setting without any known node correspondence.

Another observation is that most existing studies adopt the *one-to-one* setting of node alignment, namely, each node is matched to at most one node in the other graph.

Numerous efforts have been devoted to unsupervised graph alignment in recent years [4, 11, 44, 47, 50, 55]. One prominent category of the existing works [11, 47, 50] relies on the “*embed-then-cross-compare*” paradigm. To be more precise, these methods first learn the embedding of each node in both graphs by exploiting the graph structure and node feature information, for example, with graph neural networks (GNNs). Then, two nodes are matched if their embeddings are close according to some specific metric such as cosine similarity [50]. In other words, the intuition is to make the embeddings of two aligned nodes closer in the latent space. However, for the unsupervised scenario, it is non-trivial to design an optimization objective that is fully suitable for the graph alignment task without any known node correspondence, which poses challenges for learning high-quality embeddings. Representative embedding-based methods [11, 47] adopt the learning objective that does not directly correspond to node alignment (see Section 2.2 for more details) and employ heuristic strategies such as reweighting of graph edges [47, 50] to enable feedback in the learning process. Nonetheless, a loss that is not tailored for the specific task may lead to suboptimality of model performance. The most recent work [50] thus employs a parameter-free approach without an explicit objective to achieve state-of-the-art performance. It is obvious that the absence of supervision and a clear objective leads to the limitation of model capability under the embedding-based framework.

Another recent line of research [4, 44, 46, 55] generally models the graph alignment problem via *optimal transport (OT)*, which achieves promising accuracy due to its well-defined objective. Given the marginal distributions on two finite sets, and a predefined function named *transport cost* to describe the cost of transformation between two distributions, the OT problem finds the joint distribution to minimize the total transport cost [49]. It has been shown that unsupervised graph alignment can be reduced to OT with the help of Wasserstein discrepancy (WD) and Gromov-Wasserstein discrepancy (GWD) [32, 44, 55]. Particularly, the GW discrepancy shares similar ideas with node alignment [44, 55] given the marginals

<sup>†</sup>Corresponding author.

on both node sets, and thus, it plays a critical role in the learning process. For approaches of this paradigm, the crux lies in the cost definition between a pair of nodes, which is predefined for the OT problem but needs to be specified for graph alignment. For the well-adopted GWD, it is sufficient to define the pairwise cost within each graph (referred to as the *intra-graph cost*), then the inter-graph cost (i.e., the transport cost for OT) is computed accordingly (see Section 2.1 for more details). The advantage has been demonstrated to alleviate the effect of structure and feature inconsistency [44]. We have witnessed an increasingly sophisticated design for the concrete form of intra-graph cost, moving from hand-designed functions and learnable node embeddings [55] to node feature propagation across neighbors [44], with a combination of multiple cost terms employed by state-of-the-art algorithms [4, 44]. However, as we will elaborate in the following, to extend optimal transport to the graph alignment problem, we still lack the theoretical understanding of the added modules, i.e., the cost design and the setting of marginal distributions.

By noticing the advantages and limitations of both types of solutions, we are motivated to investigate the expressive power of OT and embedding-based techniques for unsupervised graph alignment from a more theoretical perspective. Firstly, as state-of-the-art OT-based algorithms [4, 44] essentially facilitate cost learning by node *feature propagation* on graphs, we take a step further to incorporate *feature transformation* along with propagation for intra-graph cost design. It is proved that by equipping with transformation layer, the Gromov-Wasserstein learning process gains more discriminative power, in that our cost helps to better separate matched and unmatched node pairs. Meanwhile, the provable convergence is still guaranteed under this condition.

As our empirical study shows, with this single optimization, our model outperforms existing OT and embedding-based state of the art.

Secondly, instead of proposing complicated heuristics under the embedding-based framework, which lacks a clear objective suitable for the unsupervised setting, we opt for a simple yet effective approach to improve the well-formed OT perspective by taking the embedding-based strategy as *prior knowledge*. The key observation is that existing OT-based solutions simply adapt the uniform distribution for the marginals on the node sets, while it is well known that graphs are typical non-Euclidean data and the nodes are not independent and identically distributed but associated with edges. Specifically, we use GNNs with randomized parameters to simulate the Weisfeiler-Lehman (WL) algorithm [36] and compute prior distributions for two node sets, which affects the OT-based procedure as additional inputs. We also theoretically prove that the learning process is more expressive by optimizing an orthogonal aspect to feature transformation.

Thirdly, we regret to find that none of the existing solutions guarantees the property of *one-to-one matching*. These methods are inherently incapable of satisfying the constraint because they first compute an alignment probability matrix containing the matching possibility for every pair of nodes and then take the row/column-wise maximum as the prediction. Therefore, two nodes might be aligned to the same node in the other graph as indicated by the probabilities. We tackle this problem via reducing graph alignment to the *maximum weight matching* problem [10, 18] by establishing

**Table 1: Table of notations.**

Notation	Description
$\mathcal{G}_s, \mathcal{G}_t$	The source and target graphs
$A_p, X_p$	Adjacency matrix and node feature matrix ( $p = s, t$ )
$u_i, u_j, v_k, v_l$	Nodes with $u_i, u_j \in \mathcal{G}_s$ and $v_k, v_l \in \mathcal{G}_t$
$Z_p, H_p, R_p$	Node embeddings computed by GNN, GNN w/o training, and feature propagation, respectively ( $p = s, t$ )
$C_s, C_t, C_{gwd}$	Intra-graph and inter-graph costs for GW learning
$T_{WL}, T_{GW}$	The alignment probability matrices
$f(\cdot), g(\cdot)$	Functions with and without learnable parameters

a set of weighted edges between two node sets and applying the off-the-shelf algorithms for maximum weight matching. To define the edge weights, which determine the matching accuracy, we combine the predictions of our OT and embedding-based procedures via an *ensemble learning* strategy [8, 70] named *stacking*. Our model not only holds the one-to-one matching constraint but also improves prediction accuracy by combining the best of both worlds.

Fourthly, we present a model framework named CombAlign to unify our OT and embedding-based procedures with the traditional algorithm-inspired stacking module in a principled way. Our proposed modules interact with each other to enhance alignment accuracy. Despite its more expressive power, by theoretical analysis, the asymptotic complexity of CombAlign is identical to the state-of-the-art method [44], which ensures model efficiency.

In summary, our contributions are as follows.

- We propose CombAlign, a unified framework for unsupervised graph alignment to fully integrate the advantages of embedding-based, OT-based, and traditional algorithm-based solutions.
- We enable feature transformation with learnable GNNs to enhance OT-based learning, which demonstrates more expressive power with theoretical guarantee. By formal analysis, we also observe the necessity of non-uniform marginals, and exploit prior knowledge from our embedding-based module, a simple yet effective heuristic inspired by the Weisfeiler-Lehman test.
- We use an ensemble learning strategy to unify both embedding and OT-based predictions by reducing unsupervised graph alignment to the maximum weight matching problem. To the best of our knowledge, our solution is the first to guarantee one-to-one node matching for unsupervised graph alignment.
- Extensive experiments are conducted to evaluate our algorithm against both embedding and OT-based state of the art. Our method improves the alignment accuracy by a significant margin, while a more detailed evaluation shows the effectiveness of each proposed module.

## 2 PRELIMINARIES

### 2.1 Problem Statement

We denote an undirected and attributed graph as  $\mathcal{G} = (\mathcal{V}, \mathcal{E}, \mathbf{X})$ , where the node set  $\mathcal{V}$  contains  $n$  nodes. The edge set  $\mathcal{E}$  is represented by the adjacency matrix  $\mathbf{A} \in \{0, 1\}^{n \times n}$ .  $\mathbf{X} \in \mathbb{R}^{n \times d}$  is the node feature matrix. We list frequently used notations in Table 1.

Our formal definition of the unsupervised graph alignment problem is as follows.

**Table 2: Comparison of state of the art. For GTCAIalign, the GNN parameters are randomly initialized without training.**

Method	Type	Objective Function ( $p = \{s, t\}, k \in [1, K]$ )	Main Idea	Alignment Strategy	Techniques	Time Complexity
GAlign [47]	Emb.	$\alpha \sum_p \ \tilde{A}_p^{sym} - Z_p^{(k)} Z_p^{(k)\top}\  + (1 - \alpha) \sum_{(v,v'),p} \ Z_p^{(k)}(v) - Z_p^{(k)}(v')\ $	Data augmentation-based alignment and refinement	Dot product of emb.	GNN, graph augmentation	$O(IK(md + n^2d))$
WAlign [11]	Emb.	$\alpha \sum_{(u,v)} f(Z_s(u)) - f(Z_t(v)) + (1 - \alpha) \sum_{v,p} \ f_{re}(Z_p(v)) - X_p(v)\ $	Conducting alignment via the GAN framework	Emb. similarity w.r.t. $f(\cdot)$	GNN, WGAN	$O(I(Kmd + (I_w + I_r)nd^2))$
GTCAIalign [50]	Emb.	N/A	Minimizing the angle between matched emb.	Dot product of emb.	GNN*, graph augmentation	$O(IK(md + n^2d))$
GWL [55]	OT	$\langle C_{gwd}, T \rangle + \alpha \langle C_{wd}, T \rangle + \beta L(g(X_s, X_t), C')$	Converting graph alignment to GW learning	Embedding-based WD and GWD	Proximal point method (PPM)	$O(I(n^2d + I_{ot}n^3))$
SLOTAlign [44]	OT	$\langle C_{gwd}, T \rangle$	Joint structure learning and alignment	GWD with feature propagation	Feature propagation, PPM	$O(I(K(md + nd^2) + n^2d + I_{ot}n^3))$
UHOT-GM [4]	OT	$\sum_{kk'} \alpha \langle C_{gwd}^{(kk')}, T^{(kk')} \rangle + (1 - \alpha) \langle \ X_s - X_t\ , T^{(kk')} \rangle$	Multiple and cross-modal alignment	GWD with feature propagation	Feature propagation, PPM	$O(I(K(md + nd^2) + K^2n^2d + K^2I_{ot}n^3))$

*Definition 2.1 (Unsupervised Graph Alignment).* Given source graph  $\mathcal{G}_s$  and target graph  $\mathcal{G}_t$ , unsupervised graph alignment returns a set of matched node pairs  $\mathcal{M}$ . For each node pair  $(u_i, v_k) \in \mathcal{M}$ , we have  $u_i \in \mathcal{G}_s$  and  $v_k \in \mathcal{G}_t$ .

We assume that  $n_1 = |\mathcal{V}_s|$ ,  $n_2 = |\mathcal{V}_t|$ , and  $n_1 \leq n_2$  w.l.o.g. In particular, we focus on the setting of *one-to-one* node alignment, following most existing studies [3, 4, 11, 31, 44, 47, 50, 55, 58, 61]. That is, every node can appear at most once in  $\mathcal{M}$ . One important observation is that, instead of directly computing  $\mathcal{M}$ , existing learning-based approaches [4, 11, 44, 47, 50, 55] predict an *alignment probability matrix*  $T$  of size  $n_1 \times n_2$ , where  $T(i, k)$  denotes the probability that  $u_i \in \mathcal{G}_s$  is matched to  $v_k \in \mathcal{G}_t$ . Next, it is sufficient to set  $\mathcal{M}(u_i) = \arg \max_k T(i, k)$ . In the following, we briefly discuss the concepts closely related to graph alignment.

**Gromov-Wasserstein (GW) Learning.** The discrete form of the Gromov-Wasserstein discrepancy has demonstrated its effectiveness in comparing objects across different spaces and is adopted by a wide range of machine learning tasks [13, 22], including the graph alignment problem [4, 44, 55, 61].

*Definition 2.2 (The Gromov-Wasserstein Discrepancy (GWD)).* Given the distribution  $\mu$  (resp.  $\nu$ ) over  $\mathcal{V}_s$  (resp.  $\mathcal{V}_t$ ), the GW discrepancy between  $\mu$  and  $\nu$  is defined as

$$\min_{T \in \Pi(\mu, \nu)} \sum_{i=1}^{n_1} \sum_{j=1}^{n_1} \sum_{k=1}^{n_2} \sum_{l=1}^{n_2} |C_s(i, j) - C_t(k, l)|^2 T(i, k) T(j, l), \quad (1)$$

s.t.  $T\mathbf{1} = \mu, T^\top \mathbf{1} = \nu$ .

Here,  $C_s \in \mathbb{R}^{n_1 \times n_1}$  and  $C_t \in \mathbb{R}^{n_2 \times n_2}$  are the *intra-graph costs* for  $\mathcal{G}_s$  and  $\mathcal{G}_t$ , respectively, which measure the similarity/distance of two nodes within each graph [32]. We have  $\sum_{i=1}^{n_1} \sum_{k=1}^{n_2} T(i, k) = 1$  according to the constraints in Equation 1, i.e.,  $T$  is the joint probability distribution over two node sets.

Following [32, 55], let  $C_{gwd} \in \mathbb{R}^{n_1 \times n_2}$  be the *inter-graph cost matrix*, defined as

$$C_{gwd}(i, k) = \sum_{j=1}^{n_1} \sum_{l=1}^{n_2} |C_s(i, j) - C_t(k, l)|^2 T(j, l). \quad (2)$$

The above definition of  $C_{gwd}$  can be interpreted as follows. Noticing that Equation 1 can be reformulated as

$$\langle C_{gwd}, T \rangle = \sum_{i=1}^{n_1} \sum_{k=1}^{n_2} C_{gwd}(i, k) T(i, k). \quad (3)$$

To minimize this objective with the constraints of  $T$ , a negative correlation between the values of  $C_{gwd}(i, k)$  and  $T(i, k)$  is encouraged.

More precisely, for likely matched node pairs  $(u_i, v_k)$  and  $(u_j, v_l)$ ,  $|C_s(i, j) - C_t(k, l)|^2$  should be small, i.e., the values of  $C_s(i, j)$  and  $C_t(k, l)$  are close [44, 55]. Since these intra-graph cost terms are usually computed from adjacency information and node embedding-based similarity, the GW discrepancy generally suggests that nodes with similar features and local structures are aligned.

**The Optimal Transport (OT) Problem.** Actually, Equation 3 can be interpreted via optimal transport. Given  $C \in \mathbb{R}^{n_1 \times n_2}$  which represents the cost of transforming probability distribution  $\mu$  to  $\nu$ , we compute the joint probability distribution  $T \in \mathbb{R}^{n_1 \times n_2}$  so that the total weighted cost is minimized. It can be solved by the Sinkhorn algorithm [7, 38] via an iterative procedure. Note that for optimal transport, the cost  $C$  is usually fixed (i.e., as input).

With learnable costs, existing solutions [4, 44, 55] adopt the proximal point method [54] to reduce GW learning to OT and to learn the alignment probability and parameters in the cost term jointly.

**Graph Neural Network (GNN).** To integrate the local graph structures and node features for node representation learning, one prominent approach is the graph neural networks [6, 9, 26]. To put it simply, classical GNNs compute a  $d$ -dimensional representation for each node by conducting multiple layers of graph convolution, which can be simplified as

$$Z^{(k+1)}(v) = \sigma \left( \sum_{w \in N(v)} P_{vw} \cdot Z^{(k)}(w) \cdot W^{(k+1)} \right), k = 1, \dots, K, \quad (4)$$

where  $Z^{(k)}(v)$  is  $v$ 's embedding at layer  $k$ ,  $N(v)$  denotes the neighbors of  $v$ ,  $P = g(A) \in \mathbb{R}^{n \times n}$  propagates the influence between nodes based on the graph structure,  $W^{(1)}, \dots, W^{(K)} \in \mathbb{R}^{d \times d}$  are learnable transformation matrices, and  $\sigma(\cdot)$  denotes the activation function. For example,  $P$  can be set as  $\tilde{D}^{-\frac{1}{2}} \tilde{A} \tilde{D}^{-\frac{1}{2}}$  with  $\tilde{D} = \tilde{A} \mathbf{1}$  and  $\tilde{A} = A + I$  [19, 48].

## 2.2 Analysis of State-of-the-Art Solutions

Existing unsupervised solutions for graph alignment can be roughly divided into two categories. The first category, referred to as “embed-then-cross-compare” [5, 11, 24, 47, 50, 57, 58], tackles the problem by first generating node representation (i.e., node embeddings) for both graphs. Then, the alignment probability of two nodes is computed by specific similarity measures based on their embeddings. The second category [3, 4, 31, 44, 55, 61] models graph alignment as the Gromov-Wasserstein learning process, which predicts the alignment probabilities given the transport cost between node pairs. Hence, the crux is how to design and learn the transport cost, which originates from the optimal transport problem. Table 2 shows the detailed comparison of state-of-the-art solutions.

**2.2.1 Embedding-based Solutions.** Given the embeddings of two nodes  $Z_s(u)$  and  $Z_t(v)$ , the well-adopted alignment strategy is to compute their dot product  $Z_s(u)^\top Z_t(v)$  as the matching probability [47, 50]. Note that if the embeddings are normalized, we actually minimize the cosine angle between them [50]. A more sophisticated solution [11] is to compute the node score by employing a learnable function  $f(\cdot)$ , based on which the node alignment is determined.

For node embedding computation, representative methods adopt GNN to learn the graph structures and node features jointly. Based on this, GAlign [47] incorporates the idea of data augmentation into the learning objective to obtain high-quality node embeddings. In particular, it encourages the node embeddings  $Z_p^{(k)}$  ( $p = s, t$ ) of each GNN layer  $k$  to retain graph structures, as well as to be robust upon graph perturbation (see the objective in Table 2, where  $v'$  is the node in the perturbed graph that corresponds to  $v$ ). Afterward, the alignment refinement procedure augments the original graph by first choosing the confident node matchings and then increasing the weight of their adjacency edges. This serves as an effective unsupervised heuristic to iteratively match node pairs.

GTAlign [50], which arguably has the best accuracy among embedding-based solutions, simplifies the idea of GAlign with the following observation. First, it uses a GNN with randomized parameters for node embedding computation, as it is intricate to design an embedding-based objective that directly corresponds to the goal of node alignment. Second, the iterative learning process is empowered by graph augmentation, i.e., to adjust edge weights according to confident predictions. By normalizing the node embeddings to length 1, the learning process gradually decreases the *cosine angle* between confident node matchings.

Another recent work named WAlign [11] conducts unsupervised graph alignment via the idea of generative adversarial network (GAN). Specifically, it designs a discriminator following the idea of Wasserstein GAN to minimize the distance between scores of matched node pairs, where the node score is computed from the node embedding via a learnable module (i.e., an MLP). Generally, the main challenge of embedding-based solutions lies in the absence of an objective specially tailored for graph alignment, partially due to the unsupervised setting.

**2.2.2 OT-based Solutions.** Instead of designing sophisticated alignment rules based on node embeddings, representative OT-based solutions [4, 44, 55] share the well-defined objective of minimizing Gromov-Wasserstein discrepancy (GWD) (Equation 3). Most of

them employ the proximal point method [54, 55] to solve the learning objective, which essentially models the problem via optimal transport and computes an alignment probability matrix. To this end, these methods mainly differ in the specific form of the *learnable* transport cost, which is further reduced to the intra-graph cost design. Particularly, they all adopt the joint learning process for both the cost and alignment probabilities, while the cost can be computed via predefined functions, learnable node embeddings [55], or node feature propagation [4, 44].

GWL [55] is the first work following this paradigm and incorporates Wasserstein discrepancy (WD) and reconstruction loss for regularization<sup>1</sup>. As the state-of-the-art approach, SLOAlign [44] extends GWL by incorporating multi-view structure modeling, which includes the linear combination of adjacency information, node features, and node representations computed via *feature propagation* (referred to as parameter-free GNN in [44]). A few learnable coefficients are introduced to balance their contributions to the cost. The most recent work, UHOT-GM [4], generalizes this idea with the notion of multiple and cross-modal alignment. To be specific, the node embeddings in each graph propagation layer of both graphs are fully interacted. For a  $K$ -layer propagation, it resembles conducting  $K^2$  independent GW learning procedures considering both WD [49] and GWD [44, 55], resulting in better practical accuracy.

We note that the node feature propagation in [4, 44] is fundamentally different from a parameter-free GNN, as it does not allow feature transformation (i.e., it has no transformation matrix). Therefore, the former only enables feature interaction across neighbors *dimension-by-dimension*, whereas the latter also facilitates the interaction *across* different dimensions. We will elaborate on their differences in expressive power in the following section.

**Remark.** Unfortunately, both types of solutions cannot guarantee a *one-to-one* prediction of node alignments. As the final node matchings are predicted according to the alignment probability matrix  $T$  (i.e., by finding the row/column-wise maximum), we might align both  $u_i$  and  $u_j$  in the source graph to  $v_k$  in the target graph (and vice versa), if we have  $i = \arg \max_{i'} T(i', k)$  and  $j = \arg \max_{j'} T(j', k)$ .

**2.2.3 Complexity Analysis.** We also compare the time complexity of representative solutions in Table 2. (We assume that  $\max(n_1, n_2) = O(n)$ .) Since they have common building blocks such as GNN and the GW learning procedure, their complexities also share some terms. In particular, the term  $O(K(md + nd^2))$  comes from the GNN module, while the dot product of two  $n \times d$ -sized embedding matrices takes  $O(n^2d)$  time. The cost computation of GW learning can be done in  $O(n^3)$  according to [55]. We use  $K$  to denote the number of GNN (or graph propagation) layers. All methods have the term  $I$ , which represents the number of iterations, while  $I_w$ ,  $I_r$  and  $I_{ot}$  come from the inner-loop iterations of Wasserstein discriminator [11], the reconstruction loss, and the Sinkhorn algorithm for optimal transport [4, 44, 55], respectively. In general, embedding-based methods have slightly lower asymptotic complexities. However, in practice, they tend to have comparable or longer running time than the OT-based ones (see Section 4). We speculate that the excessive time is attributed to sophisticated procedures such as graph augmentation

<sup>1</sup>In this case, GWD dominates the learning process while WD becomes one term of the transport cost.

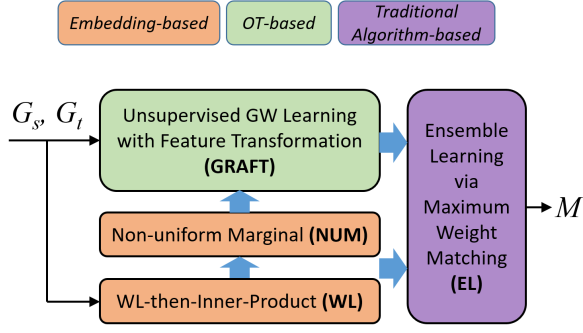


Figure 1: The overall framework of CombAlign.

and GAN, while the matrix multiplications in OT-based learning can be efficiently processed in parallel.

### 3 CombAlign: THE COMBINED APPROACH

#### 3.1 Model Overview

We present an overview of our model named CombAlign, which fully incorporates embedding-based, OT-based, and traditional techniques to solve the unsupervised graph alignment problem with theoretical improvements. The overall framework is shown in Figure 1.

Given graphs  $\mathcal{G}_s$  and  $\mathcal{G}_t$ , CombAlign (see Algorithm 1) first predicts the alignment probabilities by employing two separate approaches. Specifically, the *WL-then-Inner-Product* (WL) module obtains node embeddings  $\mathbf{H}_s$  and  $\mathbf{H}_t$  via a GNN without training, which essentially resembles the Weisfeiler-Leman (WL) algorithm (Line 1). The embedding-based alignment probability  $\mathbf{T}_{WL}$  can be easily computed by embedding-based similarity via the *Non-Uniform Marginal* (NUM) module (Line 2). Meanwhile, the *Unsupervised GW Learning with Feature Transformation* (GRAFT) module derives an OT-based prediction  $\mathbf{T}_{GW}$  by improving existing approaches [4, 44, 55] (Line 3). Also note that the NUM module has an important impact on the GRAFT module by controlling its input, i.e., the marginal distributions. Finally, the *Ensemble Learning with Maximum Weight Matching* (EL) module combines both alignment matrices and employs a traditional algorithm-based solution to further improve matching accuracy, as well as to guarantee the constraint of one-to-one matching (Lines 4-5).

---

#### Algorithm 1: CombAlign

---

**Input:** Two attributed graphs  $\mathcal{G}_s$  and  $\mathcal{G}_t$

**Output:** The set of predicted node matching  $\mathcal{M}$

- 1  $\mathbf{H}_s \leftarrow \text{WL}(\mathbf{A}_s, \mathbf{X}_s), \mathbf{H}_t \leftarrow \text{WL}(\mathbf{A}_t, \mathbf{X}_t)$ ; // Algorithm 3
  - 2  $\boldsymbol{\mu}, \boldsymbol{\nu}, \mathbf{T}_{WL} \leftarrow \text{NUM}(\mathbf{H}_s, \mathbf{H}_t)$ ; // Algorithm 4
  - 3  $\mathbf{T}_{GW} \leftarrow \text{GRAFT}(\mathbf{A}_s, \mathbf{X}_s, \mathbf{A}_t, \mathbf{X}_t, \boldsymbol{\mu}, \boldsymbol{\nu})$ ; // Algorithm 2
  - 4  $\mathcal{M} \leftarrow \text{EL}(\mathcal{V}_s, \mathcal{V}_t, \mathbf{T}_{WL}, \mathbf{T}_{GW})$ ; // Algorithm 5
  - 5
  - 6 **return**  $\mathcal{M}$ ;
- 

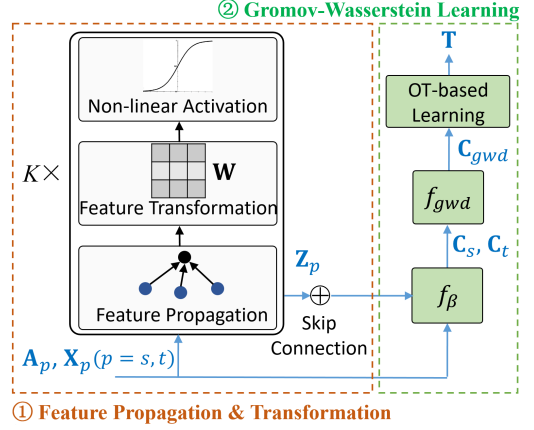


Figure 2: Illustration of the GRAFT module.

#### 3.2 The GW Learning (GRAFT) Module

We first describe the OT-based module named GRAFT (shown in Figure 2), which is composed of the feature propagation and transformation step followed by the GW learning step.

**3.2.1 Feature Propagation and Transformation.** As pointed out by [44], for OT-based approaches, the alignment quality heavily depends on the specific design of intra-graph costs  $\mathbf{C}_s$  and  $\mathbf{C}_t$ . Given the cost matrices as input, the GW learning procedure follows the standard proximal point method [54, 55] and the optimal transport solutions, e.g., the Sinkhorn algorithm [7, 38]. Consequently, apart from directly exploiting the adjacency and node feature information, representative methods [4, 44, 55] study the integration of graph structures and node features, which can be generalized as the following equation:

$$\mathbf{R}_p = g_{prop}(\mathbf{A}_p)\mathbf{X}_p, p = s, t, \quad (5)$$

where  $g_{prop}(\cdot)$  is a general function without learnable parameters. For example, we can set it to the standard propagation of GCN [19], i.e.,  $g_{prop}(\mathbf{A}_p) = \tilde{\mathbf{D}}_p^{-\frac{1}{2}} \tilde{\mathbf{A}}_p \tilde{\mathbf{D}}_p^{-\frac{1}{2}}$  (see Section 2.1). We use  $\mathbf{R}_s \in \mathbb{R}^{n_1 \times d}$  and  $\mathbf{R}_t \in \mathbb{R}^{n_2 \times d}$  to denote the result, and the process is referred to as *feature propagation*<sup>2</sup>.

We observe that this step only enables the propagation of features between a node and its neighbors in a *dimension-by-dimension* manner. However, interaction between different feature dimensions is not considered, which is also important, for example, when two feature dimensions share similar semantics. We put forward feature propagation and transformation, which is widely adopted by classical GNNs [19, 48, 56] and is formulated as

$$\mathbf{Z}_p = f_{GNN}(\mathbf{A}_p, \mathbf{X}_p, \mathbf{W}), p = s, t. \quad (6)$$

Here,  $f_{GNN}$  is a learnable function, and  $\mathbf{W}$  denotes the learnable transformation matrices and is shared by two graphs, which enables feature interaction *across dimensions*. The following theorem demonstrates that by simply adding a learnable transformation matrix for feature interaction, the intra-graph cost matrices have more discriminative power under the GW learning framework.

<sup>2</sup>Note that [44] uses parameter-free GNN to denote this process. In this paper, we propose strict definitions for both terms and formally analyze their differences.

**Theorem 3.1.** *We are given the graph structures  $\mathbf{A}_s, \mathbf{A}_t$  and node features  $\mathbf{X}_s, \mathbf{X}_t$  as input. Denote feature propagation as  $\mathbf{R}_p = g(\mathbf{A}_p)\mathbf{X}_p, p = s, t$ , where  $g(\cdot)$  is a function without learnable parameters. Denote the additional linear transformation as  $\mathbf{Z}_p = \mathbf{R}_p\mathbf{W}$ , where  $\mathbf{W} \in \mathbb{R}^{d \times d}$  is the learnable matrix. Assume that we set the intra-graph cost matrices as  $\mathbf{C}'_p = \mathbf{R}_p\mathbf{R}_p^\top$  and  $\mathbf{C}_p = \mathbf{Z}_p\mathbf{Z}_p^\top$  for  $p = s, t$ , respectively, and let  $(u_i, v_k), (u_j, v_l) \in \mathcal{M}^*$  and  $(u_{j'}, v_l) \notin \mathcal{M}^*$  where  $\mathcal{M}^*$  is the ground truth. Then, there exists a case that  $|\mathbf{C}'_s(i, j) - \mathbf{C}'_t(k, l)| = |\mathbf{C}'_s(i, j') - \mathbf{C}'_t(k, l)|$  and  $|\mathbf{C}_s(i, j) - \mathbf{C}_t(k, l)| \neq |\mathbf{C}_s(i, j') - \mathbf{C}_t(k, l)|$ .*

**PROOF.** First note that if an algorithm is able to separate  $|\mathbf{C}_s(i, j) - \mathbf{C}_t(k, l)|$  and  $|\mathbf{C}_s(i, j') - \mathbf{C}_t(k, l)|$ , or more specifically, to learn that  $|\mathbf{C}_s(i, j) - \mathbf{C}_t(k, l)| < |\mathbf{C}_s(i, j') - \mathbf{C}_t(k, l)|$ , it is more likely to make the correct prediction ( $\mathbf{T}(j, l) > \mathbf{T}(j', l)$ ). Now assume that  $\mathbf{X}_s$  contains different one-hot features for each node, and the distance between  $u_i$  and  $u_j$  (resp.  $u_{j'}$ ) is beyond  $K$ , the maximum step of feature propagation. For simplicity, let  $i, j$ , and  $j'$  be the corresponding index. Since  $u_i$  cannot propagate any information to  $u_j$  and  $u_{j'}$  (and vice versa), we have  $\mathbf{R}_s(u_i, j) = 0, \mathbf{R}_s(u_i, j') = 0, \mathbf{R}_s(u_j, i) = 0$ , and  $\mathbf{R}_s(u_{j'}, i) = 0$ . Thus, we have  $\mathbf{R}_s(u_i)^\top \mathbf{R}_s(u_j) = \mathbf{R}_s(u_i)^\top \mathbf{R}_s(u_{j'}) = 0$ , i.e.,  $\mathbf{C}'_s(i, j) = \mathbf{C}'_s(i, j') = 0$ .

With the linear transformation matrix  $\mathbf{W}$ , since the one-hot features are directly interacted, we might have  $\mathbf{Z}_s(u_i)^\top \mathbf{Z}_s(u_j) \neq 0$  and  $\mathbf{Z}_s(u_i)^\top \mathbf{Z}_s(u_{j'}) = 0$  by setting the corresponding columns of  $\mathbf{W}$ . More generally, by learning  $\mathbf{W}$ , it is possible to have  $\mathbf{Z}_s(u_i)^\top \mathbf{Z}_s(u_j) \neq \mathbf{Z}_s(u_i)^\top \mathbf{Z}_s(u_{j'})$ , and the theorem follows.  $\square$

By Theorem 3.1, if we adopt the intra-graph cost design by combining multiple terms with respect to structure and feature information [4, 44], the following corollary says that feature transformation still provides more discriminative power.

**COROLLARY 3.2.** *Assume that the intra-graph cost matrix  $\mathbf{C}_p$  is the linear combination of graph structure  $\mathbf{A}_p$ , node feature information  $\mathbf{X}_p\mathbf{X}_p^\top$ , and node embedding information  $\mathbf{Z}_p\mathbf{Z}_p^\top$ , i.e.,*

$$\mathbf{C}_p = \beta_p^{(1)}\mathbf{A}_p + \beta_p^{(2)}\mathbf{X}_p\mathbf{X}_p^\top + \beta_p^{(3)}\mathbf{Z}_p\mathbf{Z}_p^\top, p = s, t, \quad (7)$$

where we use  $\beta_p$  to represent learnable coefficients. If feature transformation is applied to compute  $\mathbf{Z}_p$ , the costs have more discriminative power in separating the matched and unmatched node pairs.

**PROOF.** Recall the example in the proof of Theorem 3.1. In this case, the first two terms of Equation 7 are equal to 0. Then the corollary holds following Theorem 3.1.  $\square$

**COROLLARY 3.3.** *Let  $\mathbf{Z}_p = f_{\text{GNN}}(\mathbf{A}_p, \mathbf{X}_p, \mathbf{W})$  denote the feature propagation and transformation step where  $f_{\text{GNN}}$  is a learnable function implemented via graph neural networks (GNNs). If  $f_{\text{GNN}}$  has more expressive power in distinguishing node embeddings, the intra-graph cost has more discriminative power in separating node pairs.*

**PROOF.** For two graphs with  $\max(n_1, n_2) = O(n)$ , note that there exists at most  $O(n)$  node matchings and  $O(n^2)$  unmatched pairs. In other words, we intend to simultaneously hold up to  $O(n^2)$  constraints described in Theorem 3.1 by learning the GNN parameters in the cost. As shown by the proof of Theorem 3.1, with a more powerful GNN to distinguish the node embeddings  $\mathbf{Z}_p$ , the intra-graph cost terms for different node pairs become more separable.  $\square$

Motivated by the above theoretical results, we employ three specific GNN models for feature propagation and transformation:

- Lightweight GCN [53] with a single linear transformation layer:

$$\mathbf{Z} = \text{Concat}(\mathbf{X}, \mathbf{P}\mathbf{X}, \dots, \mathbf{P}^K\mathbf{X})\mathbf{W}, \mathbf{P} = \tilde{\mathbf{D}}^{-\frac{1}{2}}\tilde{\mathbf{A}}\tilde{\mathbf{D}}^{-\frac{1}{2}}. \quad (8)$$

- Graph Convolutional Network (GCN) [19]:

$$\mathbf{Z}^{(k+1)} = \sigma(\mathbf{P}\mathbf{Z}^{(k)}\mathbf{W}^{(k+1)}), k \in [1, K]. \quad (9)$$

- Graph Isomorphism Network (GIN) [56]:

$$\mathbf{Z}^{(k+1)} = \text{MLP}^{(k+1)}((1 + \varepsilon^{(k+1)})\mathbf{Z}^{(k)} + \mathbf{A}\mathbf{Z}^{(k)}), k \in [1, K]. \quad (10)$$

For GCN and GIN, we use the skip connection to combine node embeddings of all layers:

$$\mathbf{Z}_p = \sum_{k=1}^K \mathbf{Z}_p^{(k)}, p = s, t. \quad (11)$$

**3.2.2 Gromov-Wasserstein Learning.** Our GW learning step follows the well-adopted approach in [4, 44, 55] by using the proximal point method and reducing the learning problem to optimal transport. Specifically, denote by  $L(\mathbf{T}, \boldsymbol{\beta}, \mathcal{W})$  the learning objective in Equation 3, where  $\boldsymbol{\beta} = (\boldsymbol{\beta}_s, \boldsymbol{\beta}_t)$  is the learnable coefficients to combine multiple terms for the intra-graph cost, and  $\mathcal{W}$  denotes the set of parameters in feature transformation. The proximal point method updates  $\mathbf{T}$  and  $\Theta = \{\boldsymbol{\beta}, \mathcal{W}\}$  alternatively [44, 55]:

$$\begin{aligned} \Theta^{(i+1)} &= \arg \min \left\{ \nabla_{\Theta} L(\mathbf{T}^{(i)}, \boldsymbol{\beta}^{(i)}, \Theta^{(i)})^\top \Theta + \frac{1}{2\tau_{\Theta}} \|\Theta - \Theta^{(i)}\|^2 \right\}, \\ \mathbf{T}^{(i+1)} &= \arg \min \left\{ \nabla_{\mathbf{T}} L(\mathbf{T}^{(i)}, \boldsymbol{\beta}^{(i)}, \Theta^{(i)})^\top \mathbf{T} + \frac{1}{\tau_{\mathbf{T}}} \text{KL}(\mathbf{T} \|\mathbf{T}^{(i)}) \right\}. \end{aligned} \quad (12)$$

Note that  $\text{KL}(\cdot \|\cdot)$  is the Kullback-Leibler divergence. Next, we demonstrate that with the simplified version of feature transformation, i.e., by adopting the lightweight GCN with one layer of linear transformation, the GW learning procedure theoretically guarantees the convergence result as in [44, 55].

**Theorem 3.4.** *Denote by  $L(\mathbf{T}, \boldsymbol{\beta}, \mathcal{W})$  the learning objective in Equation 3. Suppose that  $0 < \tau_{\mathbf{T}} < \frac{1}{L_f^{\mathbf{T}}}, 0 < \tau_{\boldsymbol{\beta}} < \frac{1}{L_f^{\boldsymbol{\beta}}}$ , and  $0 < \tau_{\mathcal{W}} < \frac{1}{L_f^{\mathcal{W}}}$ ,*

where  $L_f^{\mathbf{T}}, L_f^{\boldsymbol{\beta}}$ , and  $L_f^{\mathcal{W}}$  are the gradient Lipschitz continuous modulus of  $L(\mathbf{T}, \boldsymbol{\beta}, \mathcal{W})$  respectively. If the following conditions hold, i.e.,

$$\mathcal{T} = \{\mathbf{T} \geq 0 : \mathbf{T}\mathbf{1} = \boldsymbol{\mu}, \mathbf{T}^\top \mathbf{1} = \boldsymbol{\nu}\}, \quad (13)$$

$$\mathcal{B} = \{(\boldsymbol{\beta}_s, \boldsymbol{\beta}_t) \geq 0 : \sum_{i=1}^3 \beta_p^{(i)} = 1, p = s, t\}, \quad (14)$$

$$\mathcal{W} = \{\mathbf{W}^{(k)} \geq 0 : \sum_{i=1}^d \mathbf{W}_{ij}^{(k)} = 1, \forall j \in [1, d], k \in [1, K]\}, \quad (15)$$

then the GW learning process converges to a critical point of  $\bar{L}(\mathbf{T}, \boldsymbol{\beta}, \mathcal{W})$ , with  $\bar{L}(\mathbf{T}, \boldsymbol{\beta}, \mathcal{W}) = L(\mathbf{T}, \boldsymbol{\beta}, \mathcal{W}) + \mathbb{I}_{\mathcal{T}}(\mathbf{T}) + \mathbb{I}_{\mathcal{B}}(\boldsymbol{\beta}) + \mathbb{I}_{\mathcal{W}}(\mathcal{W})$ , where  $\mathbb{I}_{\mathcal{C}}(\cdot)$  denotes the indicator function on the set  $\mathcal{C}$ .

**PROOF (SKETCH).** Note that by our definition,  $\mathcal{T}, \mathcal{B}$ , and  $\mathcal{W}$  are bounded sets, and  $L(\mathbf{T}, \boldsymbol{\beta}, \mathcal{W})$  is a bi-quadratic function with respect to  $\mathbf{T}, \boldsymbol{\beta}$ , and  $\mathcal{W}$ . To guarantee that  $\mathcal{W}$  satisfies the above constraint in each iteration, it is sufficient to apply an activation function (e.g., ReLU) followed by column-wise normalization. The proof then

generally follows that of Theorem 5 in [44], where we can compute the gradient of  $L$  w.r.t.  $\mathbf{T}$ ,  $\boldsymbol{\beta}$ , and  $\mathcal{W}$  to update the parameters with provable convergence.  $\square$

---

**Algorithm 2:** Unsupervised Gromov-Wasserstein Learning with Feature Transformation (GRAFT)

---

**Input:**  $\mathbf{A}_s, \mathbf{X}_s, \mathbf{A}_t, \mathbf{X}_t$ , marginal distributions  $\mu$  and  $\nu$   
**Output:** The OT-based alignment probability  $\mathbf{T}_{GW}$   
 // feature propagation and transformation

- 1  $\mathbf{Z}_s^{(0)} \leftarrow \mathbf{X}_s, \mathbf{Z}_t^{(0)} \leftarrow \mathbf{X}_t$ ;
- 2 **for**  $k = 1$  to  $K$  **and**  $p = s, t$  **do**
- 3      $\mathbf{Z}_p^{(k)} \leftarrow g_{prop}(\mathbf{A}_p, \mathbf{Z}_p^{(k-1)})$ ;
- 4      $\mathbf{Z}_p^{(k)} \leftarrow \sigma(\mathbf{Z}_p^{(k)} \mathbf{W}^{(k)})$ ;
- 5  $\mathbf{Z}_s \leftarrow \sum_{k=1}^K \mathbf{Z}_s^{(k)}, \mathbf{Z}_t \leftarrow \sum_{k=1}^K \mathbf{Z}_t^{(k)}$ ;
- 6 // unsupervised Gromov-Wasserstein learning
- 6 Randomly initialize  $\mathbf{W}^{(1, \dots, K)}$  and set  $\mathbf{T}_{GW} \leftarrow \mu\nu^\top$ ,  
     $\boldsymbol{\beta}_s, \boldsymbol{\beta}_t \leftarrow (1, 1, 1)^\top$ ;
- 7 **for**  $i = 1$  to  $I$  **do**
- 8      $\mathbf{C}_p \leftarrow f_\beta(\mathbf{A}_p, \mathbf{X}_p, \mathbf{Z}_p), p = s, t$ ; // intra-graph cost
- 9      $\mathbf{C}_{gwd} \leftarrow f_{gwd}(\mathbf{C}_s, \mathbf{C}_t, \mathbf{T}_{GW})$ ; // inter-graph cost
- 10    Use (stochastic) gradient descent to update  
     $\Theta = \{\boldsymbol{\beta}, \mathbf{W}^{(1)}, \dots, \mathbf{W}^{(K)}\}$  and invoke the proximal  
    point method to update  $\mathbf{T}_{GW}$  alternatively;
- 11 **return**  $\mathbf{T}_{GW}$ ;

---

**Algorithm Description.** The pseudocode of the GRAFT module is shown in Algorithm 2. Given graph structures  $\mathbf{A}_s, \mathbf{A}_t$  and node features  $\mathbf{X}_s, \mathbf{X}_t$ , we initialize the 0-th layer embedding  $\mathbf{Z}_p^{(0)}$  as  $\mathbf{X}_p$  for  $p = s, t$  (Line 1). Next, a  $K$ -layer graph convolution is conducted (Lines 2-4) while we have multiple choices of the GNN model. We then use the skip connection to sum up embeddings of all layers and get  $\mathbf{Z}_s$  and  $\mathbf{Z}_t$  (Line 5). For the GW learning process, we randomly initialize the learnable transformation matrix  $(\mathbf{W}^{(1)}, \dots, \mathbf{W}^{(K)})$  and set the alignment probability  $\mathbf{T}_{GW}$  according to the input marginals. The learnable coefficients  $\boldsymbol{\beta}$  in the intra-graph cost are uniformly initialized (Line 6). The learning process computes the intra and inter-graph costs, and updates  $\mathbf{T}_{GW}$  by up to the maximum number of iterations (Lines 7-11).

**Remark.** Practically, we relax the theoretical constraints (Equation 14 & 15) and use more powerful GNNs to achieve better matching accuracy. Note that the objective is nonconvex and non-smooth [4, 55], and the theoretical analysis only guarantees the convergence to a critical point.

### 3.3 The WL-then-Inner-Product (WL) Module

Generally speaking, the WL module uses a GNN with randomized parameters (also referred to as *parameter-free GNNs*) to simulate the Weisfeiler-Lehman (WL) test [36]. The advantage is that the structure and feature can be embedded jointly even without an easily-defined objective. As demonstrated in Algorithm 3, we first initialize  $K$  random matrices  $\widehat{\mathbf{W}}^{(1)}, \dots, \widehat{\mathbf{W}}^{(K)}$  to resemble the hash functions in WL test (Line 1). Taking node features as input (Line 2),

the algorithm conducts  $K$  layers of graph convolution (Lines 3-4), and we get the final embeddings by summing up those in each layer (Lines 5-6). For simplicity, we use the classic GCN [19]. The only difference is that the parameters will *not* be updated. We denote by  $\mathbf{H}_s$  and  $\mathbf{H}_t$  the node representations in order to distinguish them from those obtained via a learnable GNN (i.e.,  $\mathbf{Z}_s$  and  $\mathbf{Z}_t$ ).

---

**Algorithm 3:** WL-then-Inner-Product (WL)

---

**Input:**  $\mathbf{A}_s, \mathbf{X}_s, \mathbf{A}_t, \mathbf{X}_t$   
**Output:** Node embeddings  $\mathbf{H}_s$  and  $\mathbf{H}_t$

- 1 Let  $\widehat{\mathbf{W}}^{(1)}, \dots, \widehat{\mathbf{W}}^{(K)}$  be  $K$  randomly initialized matrices;
- 2  $\mathbf{H}_s^{(0)} \leftarrow \mathbf{X}_s, \mathbf{H}_t^{(0)} \leftarrow \mathbf{X}_t$ ;
- 3 **for**  $k = 1$  to  $K$  **and**  $p = s, t$  **do**
- 4      $\mathbf{H}_p^{(k)} \leftarrow \sigma(\widetilde{\mathbf{D}}_p^{-\frac{1}{2}} \widetilde{\mathbf{A}}_p \widetilde{\mathbf{D}}_p^{-\frac{1}{2}} \cdot \mathbf{H}_p^{(k-1)} \cdot \widehat{\mathbf{W}}^{(k)})$ ;
- 5  $\mathbf{H}_s \leftarrow \sum_{k=0}^K \mathbf{H}_s^{(k)}, \mathbf{H}_t \leftarrow \sum_{k=0}^K \mathbf{H}_t^{(k)}$ ;
- 6 **return**  $\mathbf{H}_s, \mathbf{H}_t$ ;

---

Once we get the node embeddings, it is easy to compute the alignment probability by their inner product (see Section 3.4). Although the prediction of WL is not as precise as GRAFT due to its simplicity, as we will show in the following, it serves as the prior knowledge for the OT-based component to boost matching accuracy.

### 3.4 The Non-Uniform Marginal (NUM) Module

This module is for two purposes. First, given  $\mathbf{H}_s$  and  $\mathbf{H}_t$ , we compute the embedding-based alignment probability  $\mathbf{T}_{WL} \in \mathbb{R}^{n_1 \times n_2}$  by a simple dot product followed by normalization. (To guarantee its non-negativity, we first set  $\mathbf{T}_{WL} = \max(\mathbf{T}_{WL}, \mathbf{0})$ ). Second, we present a simple yet effective heuristic to improve the GRAFT module.

We observe that the OT-based component takes two marginal distributions on  $\mathcal{V}_s$  and  $\mathcal{V}_t$  as input, which is commonly assumed to be uniformly distributed [4, 44, 55]. Since graphs are typical non-Euclidean data where nodes are not i.i.d. generated, this assumption is less motivated. An illustrative example is shown in Figure 3(a). Both  $\mathcal{G}_s$  and  $\mathcal{G}_t$  contain two clusters with nodes marked as triangles and squares, respectively. We omit the edges within clusters for presentation clarity and assume that there is no edge between clusters in each graph. The nodes marked as circles denote the hubs connecting two clusters. Suppose that the correspondence between nodes is consistent with their shapes; namely, the ground truth only aligns nodes with the same shape. Note that if the pair of hubs is correctly aligned, it might eliminate a large amount of impossible alignments. In this case, a non-uniform distribution over the node set is more reasonable.

To incorporate the prior knowledge of structures and features into the GRAFT module, one strategy is to affect the marginal distributions of both graphs. We show that this observation indeed enhances the expressive power of GW learning for graph alignment.

**Theorem 3.5.** *Consider the case that  $(u_i, v_k) \in \mathcal{M}^*$  and  $(u_i, v_{k'}) \notin \mathcal{M}^*$ . For GW learning (e.g., GRAFT), under the mild assumption of the*

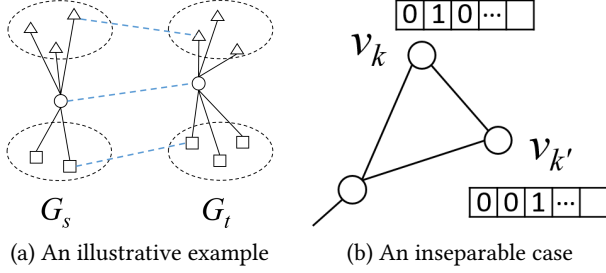
---

**Algorithm 4: Non-Uniform Marginal (NUM)**


---

**Input:** Node embeddings  $\mathbf{H}_s$  and  $\mathbf{H}_t$ 
**Output:** Two marginal distributions  $\boldsymbol{\mu}, \boldsymbol{\nu}$  and the embedding-based alignment probability  $\mathbf{T}_{WL}$ 

- 1  $\mathbf{S} \leftarrow \mathbf{H}_s \mathbf{H}_t^\top$ ;
  - 2  $\mathbf{T}_{WL} \leftarrow \mathbf{S} / \sum_{ij} S_{ij}$ ;
  - 3  $\boldsymbol{\mu} \leftarrow \mathbf{T}_{WL} \cdot \mathbf{1}, \boldsymbol{\nu} \leftarrow \mathbf{T}_{WL}^\top \cdot \mathbf{1}$ ;
  - 4 **return**  $\boldsymbol{\mu}, \boldsymbol{\nu}, \mathbf{T}_{WL}$ ;
- 


**Figure 3: Motivation of non-uniform marginals.**

intra-graph cost, i.e.,

$$C_s(i, i) = a, \forall u_i, C_t(k, k) = b, \forall v_k, \quad (16)$$

$$C_s(i, j) = C_s(j, i), C_t(k, l) = C_t(l, k), \forall u_i, u_j, v_k, v_l, \quad (17)$$

$$C_t(k, l) = C_t(k', l), \forall v_l \in \mathcal{V}_t \setminus \{v_k, v_{k'}\}, \quad (18)$$

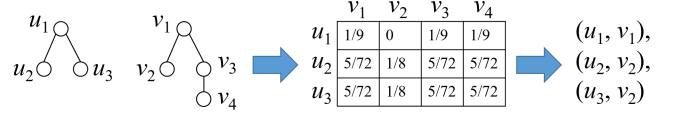
with uniform marginals  $\boldsymbol{\mu} = (1/n_1, \dots, 1/n_1)^\top$  and  $\boldsymbol{\nu} = (1/n_2, \dots, 1/n_2)^\top$ , the first iteration of the GW learning process with  $\mathbf{T}^{(0)} = \boldsymbol{\mu}\boldsymbol{\nu}^\top$  cannot determine whether  $u_i$  is matched to  $v_k$  or  $v_{k'}$ .

**PROOF.** First, we show that there exists such a case satisfying our assumption. If the embeddings in both  $\mathbf{X}_p$  and  $\mathbf{Z}_p$  are normalized, we have  $\mathbf{X}_p(v)^\top \mathbf{X}_p(v) = \mathbf{Z}_p(v)^\top \mathbf{Z}_p(v) = 1$ , thus the first constraint holds. The second constraint is satisfied for undirected graphs if each term of  $C_p$  is computed by the dot product of node embeddings. For the third constraint, refer to Figure 3(b). For two nodes  $v_k$  and  $v_{k'}$  in  $\mathcal{G}_t$  that are automorphism to each other but with different one-hot encodings, after feature propagation, we have  $\mathbf{R}_t(v_l, k) = \mathbf{R}_t(v_l, k')$  for each  $v_l$  because the propagation strategy is shared by each dimension. Therefore, we have  $\mathbf{R}_t(v_l)^\top \mathbf{R}_t(v_k) = \mathbf{R}_t(v_l)^\top \mathbf{R}_t(v_{k'})$ , and the constraint follows. Note that the above discussion also holds for feature transformation if the GNN module cannot separate  $\mathbf{Z}_t(v_l)^\top \mathbf{Z}_t(v_k)$  and  $\mathbf{Z}_t(v_l)^\top \mathbf{Z}_t(v_{k'})$ .

Second, we categorize the terms in  $C_{gwd}(i, k)$  as the following cases (Cf. Equation 2). Note that we have  $\mathbf{T}^{(0)}(i, k) = \frac{1}{n_1 n_2}, \forall i, k$ . Denote by  $c_{ik}(j, l)$  the terms in  $C_{gwd}(i, k)$ , we have

- $l = k: c_{ik}(j, k) = |C_s(i, j) - C_t(k, k)|^2 \mathbf{T}(j, k)$ ,
- $l = k': c_{ik}(j, k') = |C_s(i, j) - C_t(k, k')|^2 \mathbf{T}(j, k')$ ,
- $l \neq k, k': c_{ik}(j, l) = |C_s(i, j) - C_t(k, l)|^2 \mathbf{T}(j, l)$ .

For each  $j$ , by constraint 1 and 2, the summation of the first and second cases are equal for  $C_{gwd}(i, k)$  and  $C_{gwd}(i, k')$ . By constraint 3, for each term in the third case, the values are the same for  $v_k$  and  $v_{k'}$ . Then we have  $C_{gwd}(i, k) = C_{gwd}(i, k')$  in the first iteration of GW learning for each  $u_i \in \mathcal{G}_s$ , which completes the proof.  $\square$


**Figure 4: A toy example for one-to-many matching.**

By setting non-uniform marginals  $\boldsymbol{\mu}$  and  $\boldsymbol{\nu}$ , according to the constraint in Equation 1, the row/column-wise summation of the alignment probability prediction always follows this prior throughout the learning process. In particular, we implement the prior knowledge by the idea of WL test, and the pseudocode is shown in Algorithm 4. We compute the dot product  $\mathbf{S}$  (Line 1) and normalize it to get the embedding-based alignment probability  $\mathbf{T}_{WL}$  (Line 2). The returned marginals for GRAFT are then generated by row/column-wise summation of  $\mathbf{T}_{WL}$  (Lines 3-4). Thus, the embedding part provides prior knowledge to the OT-based part.

**Remark.** Compared to the GRAFT module, the NUM module offers another perspective to enhance the expressive power of GW learning. Recall the concrete form of  $C_{gwd}(i, k)$  in Equation 2. While GRAFT improves the discriminative power via the first part of each term, i.e.,  $|C_s(i, j) - C_t(k, l)|^2$ , NUM increases the model capability by investigating the second term  $\mathbf{T}(j, l)$ .

### 3.5 The Ensemble Learning (EL) Module

One critical drawback is observed for both embedding-based [11, 47, 50] and OT-based approaches [4, 44, 55]. Let us consider the toy example in Figure 4. Assume that the ground truth is  $\mathcal{M}^* = \{(u_i, v_i), i \in [1, 3]\}$ , and we compute the alignment probability matrix  $\mathbf{T}$  in the figure. For each  $u_i$ , we predict  $\mathcal{M}(u_i) = \arg \max_k \mathbf{T}(i, k)$ . Then, both  $u_2$  and  $u_3$  are matched to  $v_2$ . We note that this phenomenon is prevalent in real-world datasets. For representative OT and embedding-based solutions, we eliminate the one-to-many alignments by randomly keeping one of them and demonstrate the ratio of the remaining set in Figure 5. Obviously, the inability to hold the one-to-one constraint becomes a limit for model performance.

---

**Algorithm 5: Ensemble Learning via Maximum Weight Matching (EL)**


---

**Input:** Node sets  $\mathcal{V}_s$  and  $\mathcal{V}_t$ , embedding-based prediction  $\mathbf{T}_{WL}$ , OT-based prediction  $\mathbf{T}_{GW}$ 
**Output:** The refined (one-to-one) prediction  $\mathcal{M}$ 

 // build bipartite graph  $\mathcal{G}_b$  between  $\mathcal{V}_s$  and  $\mathcal{V}_t$ 

- 1  $\mathcal{V}_b \leftarrow \mathcal{V}_s \cup \mathcal{V}_t$ ;
  - 2 Construct  $\mathcal{E}_b$  by row-wise top- $r$  prediction of  $\mathbf{T}_{GW}$ ;
  - 3  $\mathcal{E}_b.weight \leftarrow g_{EL}(\mathbf{T}_{WL}, \mathbf{T}_{GW})$ ;  
// maximum weight matching
  - 4 Compute the maximum weight matching  $\mathcal{M}$  for  $\mathcal{G}_b$ ;
  - 5 **return**  $\mathcal{M}$ ;
- 

Interestingly, we find that *maximum weight matching* is a feasible solution to the problem discussed above. The maximum weight matching problem takes a bipartite graph with weighted edges as input and finds a set of edges so that their total weight is maximized, on condition that selected edges do not share any endpoint (i.e.,



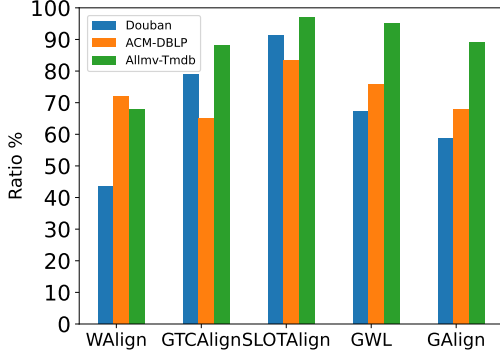


Figure 5: The ratio of the remaining set after eliminating one-to-many alignments.

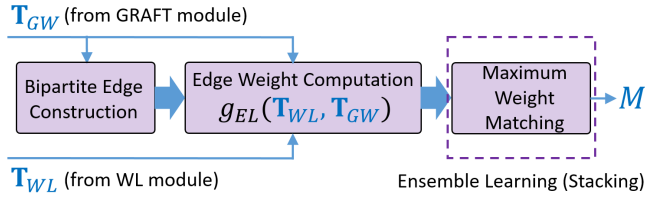


Figure 6: Illustration of the EL module.

node). The graph alignment problem can be reduced to maximum weight matching as follows. We first construct a bipartite graph from the node sets of two graphs and then establish an edge between each pair of nodes. Intuitively, the edge weight represents the probability that two adjacent nodes are aligned. To this end, finding the maximum weight matching is equivalent to graph alignment with the additional benefit of one-to-one matching.

The crux of this approach is the concrete form of the edge weight, which determines the alignment accuracy. We adopt *stacking*, an *ensemble learning* method to take the best of both worlds from OT and embedding-based predictions. In particular, we view both GRAFT and WL as base learners and form the ensemble learner via maximum weight matching. We present our EL module as follows, which is shown in Figure 6 and Algorithm 5.

**Bipartite Edge Construction.** To construct the bipartite graph  $\mathcal{G}_b$ , we set  $\mathcal{V}_b = \mathcal{V}_s \cup \mathcal{V}_t$  (Line 1 of Algorithm 5). Instead of building edges for all node pairs, we empirically observe that in most cases, the ground truth matching is contained in the top- $r$  predictions of the base learners. As the GRAFT module generally achieves better performance, for each node  $u_i \in \mathcal{G}_s$ , we connect it to the nodes in  $\mathcal{G}_t$  with top- $r$  largest  $T_{GW}(i, \cdot)$  (Line 2 of Algorithm 5). This step reduces the edge number from  $n_1 n_2$  to  $r n_1$  and significantly improves practical efficiency.

**Edge Weight Computation.** Recall that we would like the edge weight to be close to the (ground truth) alignment probability. We employ a simple yet effective *parameter-free* method to combine OT and embedding-based predictions, which is denoted as  $g_{EL}(T_{WL}, T_{GW})$  (Line 3 of Algorithm 5). We consider the following concrete forms and use the “both confident” setting by default:

- “Both learners are confident”:  $g_{EL}(T_{WL}, T_{GW}) = T_{WL} \odot T_{GW}$ ,

- “At least one is confident”:  $g_{EL}(T_{WL}, T_{GW}) = (T_{WL} + T_{GW})/2$ .

**Maximum Weight Matching.** Note that any maximum weight matching algorithm with real-value weights can be invoked to solve the problem (Line 4 of Algorithm 5). We employ the Edmonds & Karp algorithm [10, 18], which incurs  $O(n^3)$  time. Note that the algorithm returns a set of one-to-one matched node pairs instead of the alignment probability matrix (Line 5 of Algorithm 5).

The following proposition shows the effectiveness of the EL module, which is guaranteed by the property of ensemble learning.

**PROPOSITION 3.6.** *The EL module tends to obtain more accurate predictions than the embedding-based (i.e., WL) and OT-based (i.e., GRAFT) solutions.*

**Theorem 3.7.** *With the EL module, the CombAlign algorithm predicts one-to-one node alignments between  $\mathcal{V}_s$  and  $\mathcal{V}_t$ .*

**PROOF.** The conclusion is easily obtained according to the property of the maximum weight matching algorithms.  $\square$

**Complexity Analysis.** We analyze the complexity of CombAlign in brief. The WL module takes  $O(K(md + nd^2))$  time, the same as classical message-passing GNNs. The NUM module incurs  $O(n^2 d)$  because we multiply two matrices of size  $n \times d$ . The GRAFT module has the same asymptotic complexity with SLOTAAlign [44], since the additional feature transformation only needs  $O(Kd^2)$  time. For the EL module, the bipartite graph construction step takes linear time, and the complexity is dominated by the  $O(n^3)$  term of maximum weight matching. Overall, the asymptotic complexity is still  $O(I(K(md + nd^2) + n^2 d + I_{ot} n^3))$  (Cf. Table 2).

## 4 EXPERIMENTS

### 4.1 Experimental Settings

**4.1.1 Datasets.** Our experimental evaluation uses six well-adopted datasets for unsupervised graph alignment [4, 11, 44, 50, 55], including three real-world datasets Douban Online-Offline [65], ACM-DBLP [66], Allmovie-Imdb [47], as well as three synthetic ones, i.e., Cora [35], Citeseer [35], and PPI [71]. Their statistics, such as the size of both graphs, are listed in Table 3, while the anchors denote the number of ground truth matchings. The datasets relate to various domains, including social networks, collaboration networks, and protein interaction networks<sup>3</sup>. For three synthetic datasets, following all previous works, we obtain a pair of graphs by conducting node permutation of the original graph.

#### 4.1.2 Baselines and Evaluation Metrics.

**Baselines.** We compare our CombAlign algorithm with three representative embedding-based solutions, i.e., WAlign [11], GAlign [47], and GTCAlign [50], two state-of-the-art OT-based algorithms including GWL [55] and SLOTAAlign [44], along with a latest arXiv paper named UHOT-GM [4]. We choose them as baselines because WAlign and GWL are the early works of this problem with remarkable accuracy, while the other four methods have the best performance among existing approaches.

Please see Section 2.2 for more details.

<sup>3</sup>More details are referred to the full version of our paper, which is available at <https://github.com/SongyangChen2022/CombAlign>.

**Table 3: Datasets and their statistics.**

Dataset	$n_1, n_2$	$m_1, m_2$	Features	Anchors
Douban [65]	1, 118 3, 906	3, 022 16, 328	538	1, 118
ACM-DBLP [66]	9, 872 9, 916	39, 561 44, 808	17	6, 325
Allmovie-Imdb [47]	6, 011 5, 713	124, 709 119, 073	14	5, 174
Cora [35]	2, 708 2, 708	5, 028 5, 028	1, 433	2, 708
Citeseer [35]	3, 327 3, 327	4, 732 4, 732	3, 703	3, 327
PPI [71]	1, 767 1, 767	16, 159 16, 159	50	1, 767

For all baselines except UHOT-GM, we obtain the codes from the authors. We report the performance of UHOT-GM according to its latest arXiv version. All experiments are conducted on a high-performance computing server with a GeForce RTX 4090 GPU.

**Evaluation Metrics.** We adopt Hits@ $k$  with  $k = \{1, 5, 10\}$  following most previous studies. Given the ground truth  $\mathcal{M}^*$ , for each  $(u, v) \in \mathcal{M}^*$  with  $u \in \mathcal{G}_s$  and  $v \in \mathcal{G}_t$ , we check if  $v$  belongs to the top- $k$  predictions ordered by alignment probability, denoted as  $S_k(u)$ . Then, Hits@ $k$  is computed as follows:

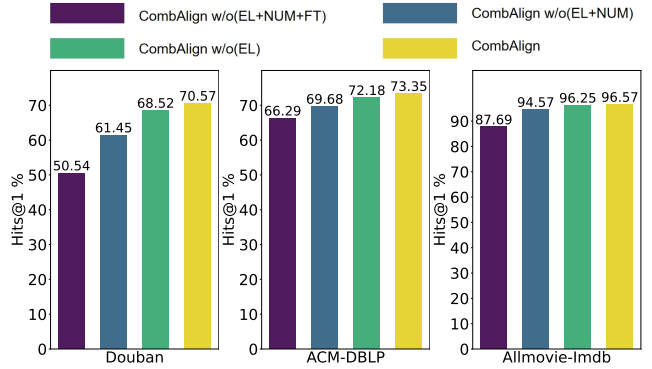
$$\text{Hits}@k = \frac{\sum_{(u,v) \in \mathcal{M}^*} \mathbb{1}[v \in S_k(u)]}{|\mathcal{M}^*|}, \quad (19)$$

where  $\mathbb{1}[\cdot]$  is the indicator function which equals 1 if the condition holds. Particularly, we focus on Hits@1, which is essentially the alignment accuracy. We omit other metrics such as mean average precision (MAP) for space limit, as the performance w.r.t. both metrics are consistent. Please refer to the full paper for more details.

## 4.2 Experimental Results

**4.2.1 Overall Performance.** The matching accuracy of each method is demonstrated in Table 4. We use the bold font to highlight the best result and underline the second-best values. The reported figures are the average of five independent rounds, and we omit the standard errors following most existing works because the prediction accuracy is highly concentrated for this problem. Among the embedding and OT-based algorithms for comparison, note that GAlign achieves the best performance on ACM-DBLP while SLOTAI<sub>gn</sub> has the highest accuracy on Allmovie-Imdb. For the Douban dataset, GTCAI<sub>gn</sub> and UHOT-GM are the two best baselines. It can be concluded that neither OT-based methods nor embedding solutions can consistently outperform the other.

Meanwhile, for the embedding-based algorithms, we note that there does not exist a clear winner between GAlign and GTCAI<sub>gn</sub> on the real-world datasets, demonstrating the limitation of the embedding-only heuristics in the unsupervised setting. Nonetheless, both of them outperform WAI<sub>gn</sub>, while the training process of the latter encounters significant oscillations, partially due to the challenges in training GANs [1, 12]. For the OT-based methods,

**Figure 7: Ablation study on three real-world datasets.**

it is clear that more sophisticated design of intra-graph costs by considering multiple terms (i.e., SLOTAI<sub>gn</sub>) and cross-modal comparison (i.e., UHOT-GM) results in better practical accuracy. This not only demonstrates the importance of intra-graph cost design but also proves that feature propagation is a more powerful tool than node feature similarity and hand-crafted cost functions.

For our CombAlign algorithm, it consistently achieves the best performance for all values of  $k$  on all three real-world datasets. In terms of Hits@1, i.e., the alignment accuracy, our improvements over the best baseline are 12.1%, 4.5% and 6.6% for Douban, ACM-DBLP, and Allmovie-Imdb, respectively. For the synthetic datasets, CombAlign also has the highest performance except for Hits@10 on PPI.

Though most baselines achieve performance close to 100% on Cora and Citeseer for Hits@1, CombAlign manages to further reduce this gap.

**4.2.2 Ablation Study.** To test the effectiveness of each module, we progressively remove EL, NUM, and feature transformation in GRAFT. The resulting model variants are as follows. For CombAlign w/o EL, we predict  $\mathcal{M}$  via  $T_{GW}$  because it generally achieves higher accuracy by combining the prior knowledge from NUM. CombAlign w/o EL+NUM further eliminates the NUM and WL modules, therefore, the uniform marginal is adopted. The CombAlign w/o EL+NUM+FT variant removes feature transformation as well as feature propagation, resulting in a model theoretically weaker than SLOTAI<sub>gn</sub>.

We show the results of the ablation study in Figure 7. It is clear that all proposed modules have non-negligible contributions to model accuracy. More specifically, EL boosts the accuracy on Douban (resp. ACM-DBLP) by more than two (resp. one) points. Notably, the non-uniform marginal and feature transformation significantly increase the performance of CombAlign. For CombAlign w/o EL+NUM+FT, the accuracy is close to SLOTAI<sub>gn</sub>, which coincides with the fact that the two models have minor differences.

**4.2.3 Evaluation of Different Modules.** We conduct a more extensive investigation of the proposed modules. First, we incorporate different GNN models into GRAFT. According to the theoretical results of Corollary 3.3, more expressive GNNs should lead to better model accuracy. As shown in Table 5, we employ the CombAlign

**Table 4: Comparison of model performance on six datasets.**

Datasets	Metrics	GAlign	WAlign	GTCAlign	GWL	SLOTAlign	UHOT-GM	CombAlign
Douban Online-Offline	Hits@1	45.26	39.45	61.79	3.29	51.43	<u>62.97</u>	<b>70.57</b>
	Hits@5	67.71	62.35	<u>76.83</u>	8.32	73.43	71.47	<b>87.84</b>
	Hits@10	78.00	71.47	<u>82.29</u>	9.93	77.73	75.76	<b>91.41</b>
ACM-DBLP	Hits@1	<u>70.20</u>	63.43	60.92	56.36	66.04	69.53	<b>73.35</b>
	Hits@5	<u>87.23</u>	83.18	75.60	77.09	85.84	86.97	<b>88.98</b>
	Hits@10	<u>91.36</u>	86.58	79.97	82.18	87.76	90.26	<b>92.63</b>
Allmovie-Imdb	Hits@1	82.14	52.61	84.73	87.82	<u>90.60</u>	-	<b>96.57</b>
	Hits@5	86.35	70.91	89.89	92.31	<u>92.75</u>	-	<b>97.66</b>
	Hits@10	90.03	76.52	91.32	92.83	<u>93.14</u>	-	<b>97.89</b>
Cora	Hits@1	99.45	98.45	99.35	86.19	<u>99.48</u>	99.41	<b>99.56</b>
	Hits@5	<b>100</b>	<b>100</b>	<b>100</b>	93.61	<b>100</b>	<b>100</b>	<b>100</b>
	Hits@10	<b>100</b>	<b>100</b>	<b>100</b>	94.57	<b>100</b>	<b>100</b>	<b>100</b>
Citeseer	Hits@1	<u>99.73</u>	97.81	99.68	57.05	99.25	-	<b>99.82</b>
	Hits@5	<b>100</b>	<b>100</b>	<b>100</b>	65.04	<b>100</b>	-	<b>100</b>
	Hits@10	<b>100</b>	<b>100</b>	<b>100</b>	65.95	<b>100</b>	-	<b>100</b>
PPI	Hits@1	89.20	88.51	89.25	86.76	<u>89.30</u>	87.10	<b>89.70</b>
	Hits@5	90.64	<u>93.10</u>	92.81	88.06	92.53	91.06	<b>93.15</b>
	Hits@10	<u>94.16</u>	<b>94.17</b>	94.07	88.62	93.49	92.13	93.85

**Table 5: The performance of GRAFT with different GNNs for Hits@1.**

	Douban	ACM-DBLP	Allmovie-Imdb
GRAFT w/ LGCN	57.07	68.87	93.39
GRAFT w/ GCN	61.45	69.68	94.57
GRAFT w/ GIN	<b>63.15</b>	<b>71.64</b>	<b>95.61</b>

w/o EL+NUM variant to test the lightweight GCN, GCN, and GIN (Cf. Section 3.2). The result nicely matches our theoretical conclusion.

Note that by default the GRAFT module uses GCN (e.g., for Table 4). We also point out that the GIN variant in Table 5 has already outperformed all baselines shown in Table 4. We believe there is still room for further improvements with more powerful GNNs.

Second, we validate the one-to-one matching property of the EL module. For the model variants of CombAlign, we show the ratio of the remaining set compared to the ground truth set after eliminating one-to-many predictions. This step is the same as in Figure 5 (see Section 3.5), in which we demonstrate the ratio of our baselines (except for UHOT-GM). Recall that even with EL, the result size of CombAlign might still be smaller than the ground truth. This is because the maximum weight matching of two graphs with  $n$  nodes (and without complete bipartite edges) typically gives less than  $n$  matched pairs. However, the performance on Douban and Allmovie-Imdb is remarkable. It can be seen that the ratio is generally consistent with model accuracy, and our results significantly outperform the baselines in Figure 5.

Third, the two different ensemble strategies (Cf. Sections 3.5) are evaluated, namely, “both confident” and “at least one being confident”. It turns out that “both confident”, the most intuitive strategy,

**Table 6: The ratio of the remaining set over  $|M^*|$  after eliminating one-to-many predictions.**

	Douban	ACM-DBLP	Allmovie-Imdb
CombAlign	<b>99.70%</b>	<b>94.57%</b>	<b>100%</b>
- w/o EL	94.18%	88.36%	98.54%
- w/o EL+NUM	94.36%	86.50%	97.60%
- w/o EL+NUM+FT	91.32%	83.27%	96.25%

**Table 7: The performance of different ensemble strategies in terms of Hits@1.**

	Douban	ACM-DBLP	Allmovie-Imdb
$(T_{WL} + T_{GW})/2$	66.90	72.86	<b>96.57</b>
$T_{WL} \odot T_{GW}$	<b>70.57</b>	<b>73.35</b>	<b>96.57</b>

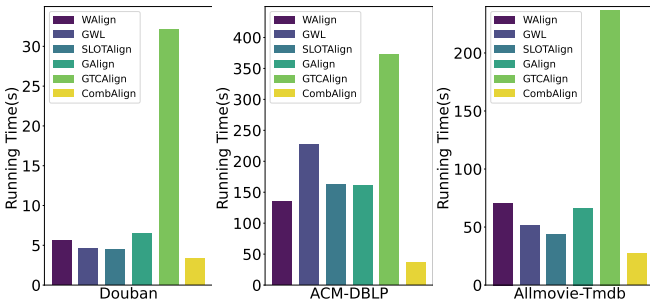
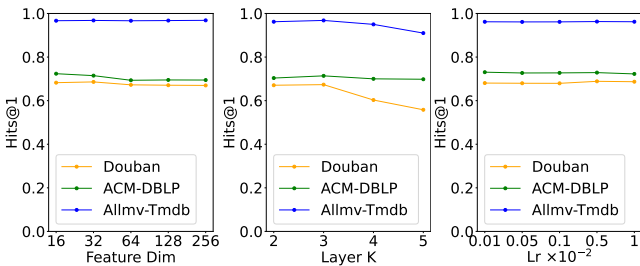
has better performance, which is our default setting. However, the other setting is still comparable in most cases. It is interesting to study other strategies of ensemble learning in future work.

Fourth, we use the idea of ensemble learning to enhance existing OT-based solutions. We substitute the GRAFT module with GWL and SLOTAlign, and use the final prediction of EL. The result is illustrated in Table 8. Both methods obtain a significant enhancement of Hits@1 on three real-world datasets.

**4.2.4 Model Efficiency.** We compare the running time of all algorithms in Figure 8. The model accuracy generally converges except for WAlign. Note that all baselines, as well as the GRAFT, WL, and NUM modules, run on the GPU. While the EL module, which acts as the post-processing step, resides in the CPU. Therefore, we report the running time of CombAlign w/o EL, which also outperforms the

**Table 8: Improving other OT-based models with EL. (Hits@1 is demonstrated.)**

	Douban	ACM-DBLP	Allmovie-Imdb
GWL	3.29	56.36	87.82
GWL+EL	5.81	63.46	90.07
SLOTAlign	51.43	66.04	90.60
SLOTAlign+EL	60.01	69.20	91.03


**Figure 8: Running time of different methods. The time of CombAlign w/o EL is reported.**

**Figure 9: Impact of hyper-parameters on CombAlign.**

baselines by a significant margin. Generally speaking, all baselines have comparable running times apart from GTCAlign. We speculate that the sophisticated graph augmentation in each iteration is time-costly. For our method, the running time is low because fewer iterations are needed, partially due to its more expressiveness. We leave the parallelization of maximum weight matching algorithms as future work.

**4.2.5 Sensitivity Analysis.** To examine the impact of different hyper-parameters on our model, experiments are conducted for feature dimension  $d$ , the number of graph convolution layers  $K$ , and the learning rate. In general, the model performance is stable w.r.t.  $d$ .

Meanwhile, the accuracy declines when  $K$  exceeds 3, consistent with the oversmoothing problem of GNNs. This phenomenon is more pronounced for Douban because one graph is very sparse. Our model is robust for a wide range of learning rates.

## 5 OTHER RELATED WORK

**Unsupervised Graph Alignment.** Earlier works for the unsupervised setting focus on the consistency principle [65] and adopt

various methods including matrix factorization [15, 16], locality sensitive hashing [14], and random walk with restart (RWR) based feature propagation [65]. The research focus then gradually moves on to embedding-based [5, 11, 24, 29, 30, 40, 47, 50, 58] and optimal transport-based solutions [4, 44, 46, 55] for better model capability. Refer to Section 2.2 for a more detailed discussion of recent studies. **Supervised Graph Alignment.** With a set of anchor node pairs as input, the main idea of supervised methods is to fully utilize the anchor information. A line of consistency-based algorithms [20, 37, 62, 65, 67] is proposed to first define the neighborhood topology and attribute consistency followed by devising a procedure to propagate the anchor information across graphs, e.g., via RWR. Follow-up works resort to embedding-based approaches [5, 15, 17, 58, 68, 69], i.e., by learning node embeddings to make the anchor pairs close while preserving the graph structure in the latent space. A very recent work [61] incorporates the idea of optimal transport to better model the alignment consistency. Along with the RWR-based transport cost design, state-of-the-art performance is achieved.

**Knowledge Graph (KG) Entity Alignment.** We also note that a similar problem has been extensively studied [41, 42, 51, 52, 60], which aligns the entities across knowledge graphs [64]. For this problem setting, both topological structures and the semantics of features are important. Existing literature can be roughly categorized into the traditional heuristics [34, 39], the self-supervised methods [25, 59], and some optimization-based solutions [27, 28]. The up-to-date study [45] employs optimal transport and proposes a fused WD and GWD framework to tackle this problem.

## 6 CONCLUSION

We propose CombAlign, a unified model framework to combine the advantages of embedding-based, optimal transport (OT)-based, and traditional algorithm-based techniques. Our model consists of GRAFT, the OT-based module which has a well-defined learning objective and is enhanced by feature transformation. The two embedding-based modules, WL and NUM, use a simple yet effective heuristic for alignment probability prediction and then provide prior knowledge to GRAFT. The EL module is considered as the post-processing step to reduce graph alignment to maximum weight matching following the idea of stacking, an ensemble learning technique. Our proposed modules are equipped with theoretical guarantees of more expressiveness, including more discriminative power and one-to-one matching. The effectiveness of our model is confirmed by extensive experiments.

## REFERENCES

- [1] Martín Arjovsky, Soumith Chintala, and Léon Bottou. 2017. Wasserstein Generative Adversarial Networks. In *Proceedings of the 34th International Conference on Machine Learning, ICML 2017, Sydney, NSW, Australia, 6–11 August 2017*.
- [2] Florian Bernard, Johan Thunberg, Peter Gemmar, Frank Hertel, Andreas Husch, and Jorge Goncalves. 2015. A solution for multi-alignment by transformation synchronisation. In *Proceedings of the IEEE conference on computer vision and pattern recognition*. 2161–2169.
- [3] Liqun Chen, Zhe Gan, Yu Cheng, Linjie Li, Lawrence Carin, and Jingjing Liu. 2020. Graph optimal transport for cross-domain alignment. In *International Conference on Machine Learning*. PMLR, 1542–1553.
- [4] Haoran Cheng, Dixin Luo, and Hongteng Xu. 2023. DHOT-GM: Robust Graph Matching Using A Differentiable Hierarchical Optimal Transport Framework. *arXiv preprint arXiv:2310.12081* (2023).
- [5] Xiaokai Chu, Xinxin Fan, Di Yao, Zhihua Zhu, Jianhui Huang, and Jingping Bi. 2019. Cross-network embedding for multi-network alignment. In *The world wide web conference*. 273–284.
- [6] Gabriele Corso, Hannes Stark, Stefanie Jegelka, Tommi Jaakkola, and Regina Barzilay. 2024. Graph neural networks. *Nature Reviews Methods Primers* 4, 1 (2024), 17.
- [7] Marco Cuturi. 2013. Sinkhorn distances: Lightspeed computation of optimal transport. *Advances in neural information processing systems* 26 (2013).
- [8] Thomas G Dietterich. 2000. Ensemble methods in machine learning. In *International workshop on multiple classifier systems*. Springer, 1–15.
- [9] Chi Thang Duong, Trung Dung Hoang, Hongzhi Yin, Matthias Weidlich, Quoc Viet Hung Nguyen, and Karl Aberer. 2021. Efficient streaming subgraph isomorphism with graph neural networks. *Proceedings of the VLDB Endowment* 14, 5 (2021), 730–742.
- [10] Jack Edmonds and Richard M Karp. 1972. Theoretical improvements in algorithmic efficiency for network flow problems. *Journal of the ACM (JACM)* 19, 2 (1972), 248–264.
- [11] Ji Gao, Xiao Huang, and Jundong Li. 2021. Unsupervised graph alignment with wasserstein distance discriminator. In *Proceedings of the 27th ACM SIGKDD Conference on Knowledge Discovery & Data Mining*. 426–435.
- [12] Ishaan Gulrajani, Faruk Ahmed, Martin Arjovsky, Vincent Dumoulin, and Aaron C Courville. 2017. Improved training of wasserstein gans. *Advances in neural information processing systems* 30 (2017).
- [13] Stefan Haller, Lorenz Feineis, Lisa Hutschenreiter, Florian Bernard, Carsten Rother, Dagmar Kainmüller, Paul Swoboda, and Bogdan Savchynskyy. 2022. A comparative study of graph matching algorithms in computer vision. In *European Conference on Computer Vision*. Springer, 636–653.
- [14] Mark Heimann, Wei Lee, Shengjie Pan, Kuan-Yu Chen, and Danai Koutra. 2018. Hashalign: Hash-based alignment of multiple graphs. In *Advances in Knowledge Discovery and Data Mining: 22nd Pacific-Asia Conference, PAKDD 2018, Melbourne, VIC, Australia, June 3–6, 2018, Proceedings, Part III 22*. Springer, 726–739.
- [15] Mark Heimann, Haoming Shen, Tara Safavi, and Danai Koutra. 2018. Regal: Representation learning-based graph alignment. In *Proceedings of the 27th ACM international conference on information and knowledge management*. 117–126.
- [16] Judith Hermanns, Anton Tsitsulin, Marina Munkhoeva, Alex Bronstein, Davide Mottin, and Panagiotis Karras. 2021. Grasp: Graph alignment through spectral signatures. In *Web and Big Data: 5th International Joint Conference, APWeb-WAIM 2021, Guangzhou, China, August 23–25, 2021, Proceedings, Part I 5*. Springer, 44–52.
- [17] Huiting Hong, Xin Li, Yuqiang Pan, and Ivor W Tsang. 2020. Domain-adversarial network alignment. *IEEE Transactions on Knowledge and Data Engineering* 34, 7 (2020), 3211–3224.
- [18] Roy Jonker and Ton Volgenant. 1988. A shortest augmenting path algorithm for dense and sparse linear assignment problems. In *DGOR/NSOR: Papers of the 16th Annual Meeting of DGOR in Cooperation with NSOR/Vorträge der 16. Jahrestagung der DGOR zusammen mit der NSOR*. Springer, 622–622.
- [19] Thomas N Kipf and Max Welling. 2016. Semi-supervised classification with graph convolutional networks. *arXiv preprint arXiv:1609.02907* (2016).
- [20] Danai Koutra, Hanghang Tong, and David Lubensky. 2013. Big-align: Fast bipartite graph alignment. In *2013 IEEE 13th international conference on data mining*. IEEE, 389–398.
- [21] Chaozhuo Li, Senzhang Wang, Hao Wang, Yanbo Liang, Philip S Yu, Zhoujun Li, and Wei Wang. 2019. Partially shared adversarial learning for semi-supervised multi-platform user identity linkage. In *Proceedings of the 28th ACM international conference on information and knowledge management*. 249–258.
- [22] Xiucheng Li, Gao Cong, Aixin Sun, and Yun Cheng. 2019. Learning travel time distributions with deep generative model. In *World Wide Web Conference*. 1017–1027.
- [23] Junfeng Liu, Min Zhou, Shuai Ma, and Lujia Pan. 2023. MATA<sup>+</sup>: Combining Learnable Node Matching with A<sup>+</sup> Algorithm for Approximate Graph Edit Distance Computation. *arXiv:2311.02356 [cs.LG]*
- [24] Li Liu, William K Cheung, Xin Li, and Lejian Liao. 2016. Aligning Users across Social Networks Using Network Embedding. In *Ijcai*, Vol. 16. 1774–80.
- [25] Xiao Liu, Haoyun Hong, Xinghao Wang, Zeyi Chen, Evgeny Kharlamov, Yuxiao Dong, and Jie Tang. 2022. Selfkg: Self-supervised entity alignment in knowledge graphs. In *Proceedings of the ACM Web Conference 2022*. 860–870.
- [26] Ge Lv and Lei Chen. 2023. On Data-Aware Global Explainability of Graph Neural Networks. *Proceedings of the VLDB Endowment* 16, 11 (2023), 3447–3460.
- [27] Xin Mao, Wenting Wang, Yuanbin Wu, and Man Lan. 2021. From alignment to assignment: Frustratingly simple unsupervised entity alignment. *arXiv preprint arXiv:2109.02363* (2021).
- [28] Xin Mao, Wenting Wang, Yuanbin Wu, and Man Lan. 2022. Lightea: A scalable, robust, and interpretable entity alignment framework via three-view label propagation. *arXiv preprint arXiv:2210.10436* (2022).
- [29] Jin-Duk Park, Cong Tran, Won-Yong Shin, and Xin Cao. 2022. Grad-Align: Gradual network alignment via graph neural networks (Student Abstract). In *Proceedings of the AAAI conference on artificial intelligence*, Vol. 36. 13027–13028.
- [30] Jingkai Peng, Fei Xiong, Shirui Pan, Liang Wang, and Xi Xiong. 2023. Robust Network Alignment with the Combination of Structure and Attribute Embeddings. In *2023 IEEE International Conference on Data Mining (ICDM)*. IEEE, 498–507.
- [31] Hermina Petric Maretic, Mireille El Gheche, Giovanni Chierchia, and Pascal Frossard. 2019. GOT: an optimal transport framework for graph comparison. *Advances in Neural Information Processing Systems* 32 (2019).
- [32] Gabriel Peyré, Marco Cuturi, and Justin Solomon. 2016. Gromov-wasserstein averaging of kernel and distance matrices. In *International conference on machine learning*. PMLR, 2664–2672.
- [33] Chengzhi Piao, Tingyang Xu, Xiangguo Sun, Yu Rong, Kangfei Zhao, and Hong Cheng. 2023. Computing Graph Edit Distance via Neural Graph Matching. *Proceedings of the VLDB Endowment* 16, 8 (2023), 1817–1829.
- [34] Zhiyuan Qi, Ziheng Zhang, Jiaoyan Chen, Xi Chen, Yuejia Xiang, Ningyu Zhang, and Yefeng Zheng. 2021. Unsupervised knowledge graph alignment by probabilistic reasoning and semantic embedding. *arXiv preprint arXiv:2105.05596* (2021).
- [35] Prithviraj Sen, Galileo Namata, Mustafa Bilgic, Lise Getoor, Brian Galligher, and Tina Eliassi-Rad. 2008. Collective classification in network data. *AI magazine* 29, 3 (2008), 93–93.
- [36] Nino Shervashidze, Pascal Schweitzer, Erik Jan Van Leeuwen, Kurt Mehlhorn, and Karsten M Borgwardt. 2011. Weisfeiler-lehman graph kernels. *Journal of Machine Learning Research* 12, 9 (2011).
- [37] Rohit Singh, Jinbo Xu, and Bonnie Berger. 2008. Global alignment of multiple protein interaction networks with application to functional orthology detection. *Proceedings of the National Academy of Sciences* 105, 35 (2008), 12763–12768.
- [38] Richard Sinkhorn and Paul Knopp. 1967. Concerning nonnegative matrices and doubly stochastic matrices. *Pacific J. Math.* 21, 2 (1967), 343–348.
- [39] Fabian M Stachanek, Serge Abiteboul, and Pierre Senellart. 2011. Paris: Probabilistic alignment of relations, instances, and schema. *arXiv preprint arXiv:1111.7164* (2011).
- [40] Qingqiang Sun, Xuemin Lin, Ying Zhang, Wenjie Zhang, and Chaoqi Chen. 2023. Towards higher-order topological consistency for unsupervised network alignment. In *2023 IEEE 39th International Conference on Data Engineering (ICDE)*. IEEE, 177–190.
- [41] Zequn Sun, Wei Hu, Qingheng Zhang, and Yuzhong Qu. 2018. Bootstrapping entity alignment with knowledge graph embedding. In *IJCAI*, Vol. 18.
- [42] Zequn Sun, Chengming Wang, Wei Hu, Muhao Chen, Jian Dai, Wei Zhang, and Yuzhong Qu. 2020. Knowledge graph alignment network with gated multi-hop neighborhood aggregation. In *Proceedings of the AAAI conference on artificial intelligence*, Vol. 34. 222–229.
- [43] Jie Tang, Jing Zhang, Limin Yao, Juanzi Li, Li Zhang, and Zhong Su. 2008. Arnetminer: extraction and mining of academic social networks. In *Proceedings of the 14th ACM SIGKDD international conference on Knowledge discovery and data mining*. 990–998.
- [44] Jianheng Tang, Weiqi Zhang, Jiabin Li, Kangfei Zhao, Fugee Tsung, and Jia Li. 2023. Robust attributed graph alignment via joint structure learning and optimal transport. In *2023 IEEE 39th International Conference on Data Engineering (ICDE)*. IEEE, 1638–1651.
- [45] Jianheng Tang, Kangfei Zhao, and Jia Li. 2023. A fused gromov-wasserstein framework for unsupervised knowledge graph entity alignment. *arXiv preprint arXiv:2305.06574* (2023).
- [46] Vayer Titouan, Nicolas Courty, Romain Tavenard, and Rémi Flamary. 2019. Optimal transport for structured data with application on graphs. In *International Conference on Machine Learning*. PMLR, 6275–6284.
- [47] Huynh Thanh Trung, Tong Van Vinh, Nguyen Thanh Tam, Hongzhi Yin, Matthias Weidlich, and Nguyen Quoc Viet Hung. 2020. Adaptive network alignment with unsupervised and multi-order convolutional networks. In *2020 IEEE 36th International Conference on Data Engineering (ICDE)*. IEEE, 85–96.
- [48] Petar Veličković, Guillem Cucurull, Arantxa Casanova, Adriana Romero, Pietro Lio, and Yoshua Bengio. 2017. Graph attention networks. *arXiv preprint arXiv:1710.10903* (2017).
- [49] Cédric Villani et al. 2009. *Optimal transport: old and new*. Vol. 338.
- [50] Chenxu Wang, Peijing Jiang, Xiangliang Zhang, Pinghui Wang, Tao Qin, and Xiaohong Guan. 2023. GTCAalign: Global Topology Consistency-based Graph

- Alignment. *IEEE Transactions on Knowledge and Data Engineering* (2023).
- [51] Zhichun Wang, Qingsong Lv, Xiaohan Lan, and Yu Zhang. 2018. Cross-lingual knowledge graph alignment via graph convolutional networks. In *Proceedings of the 2018 conference on empirical methods in natural language processing*. 349–357.
- [52] Zhichun Wang, Jinjian Yang, and Xiaoju Ye. 2020. Knowledge graph alignment with entity-pair embedding. In *Proceedings of the 2020 Conference on Empirical Methods in Natural Language Processing (EMNLP)*. 1672–1680.
- [53] Felix Wu, Amauri Souza, Tianyi Zhang, Christopher Fifty, Tao Yu, and Kilian Weinberger. 2019. Simplifying graph convolutional networks. In *International conference on machine learning*. PMLR, 6861–6871.
- [54] Yujia Xie, Xiangfeng Wang, Ruijia Wang, and Hongyuan Zha. 2020. A fast proximal point method for computing exact wasserstein distance. In *Uncertainty in artificial intelligence*. PMLR, 433–453.
- [55] Hongteng Xu, Dixin Luo, Hongyuan Zha, and Lawrence Carin Duke. 2019. Gromov-wasserstein learning for graph matching and node embedding. In *International conference on machine learning*. PMLR, 6932–6941.
- [56] Keyulu Xu, Weihua Hu, Jure Leskovec, and Stefanie Jegelka. 2018. How powerful are graph neural networks? *arXiv preprint arXiv:1810.00826* (2018).
- [57] Yuchen Yan, Lihui Liu, Yikun Ban, Baoyu Jing, and Hanghang Tong. 2021. Dynamic knowledge graph alignment. In *Proceedings of the AAAI conference on artificial intelligence*, Vol. 35. 4564–4572.
- [58] Yuchen Yan, Si Zhang, and Hanghang Tong. 2021. Bright: A bridging algorithm for network alignment. In *Proceedings of the web conference 2021*. 3907–3917.
- [59] Kaisheng Zeng, Zhenhao Dong, Lei Hou, Yixin Cao, Minghao Hu, Jifan Yu, Xin Lv, Lei Cao, Xin Wang, Haozhuang Liu, et al. 2022. Interactive contrastive learning for self-supervised entity alignment. In *Proceedings of the 31st ACM International Conference on Information & Knowledge Management*. 2465–2475.
- [60] Kaisheng Zeng, Chengjiang Li, Lei Hou, Juanzi Li, and Ling Feng. 2021. A comprehensive survey of entity alignment for knowledge graphs. *AI Open* 2 (2021), 1–13.
- [61] Zhichen Zeng, Si Zhang, Yinglong Xia, and Hanghang Tong. 2023. PARROT: Position-Aware Regularized Optimal Transport for Network Alignment. In *Proceedings of the ACM Web Conference 2023*. 372–382.
- [62] Jiawei Zhang and S Yu Philip. 2015. Integrated anchor and social link predictions across social networks. In *Twenty-fourth international joint conference on artificial intelligence*.
- [63] Jiawei Zhang and S Yu Philip. 2015. Multiple anonymized social networks alignment. In *2015 IEEE International Conference on Data Mining*. IEEE, 599–608.
- [64] Rui Zhang, Bayu Distiawan Trisedya, Miao Li, Yong Jiang, and Jianzhong Qi. 2022. A benchmark and comprehensive survey on knowledge graph entity alignment via representation learning. *The VLDB Journal* 31, 5 (2022), 1143–1168.
- [65] Si Zhang and Hanghang Tong. 2016. Final: Fast attributed network alignment. In *Proceedings of the 22nd ACM SIGKDD international conference on knowledge discovery and data mining*. 1345–1354.
- [66] Si Zhang and Hanghang Tong. 2018. Attributed network alignment: Problem definitions and fast solutions. *IEEE Transactions on Knowledge and Data Engineering* 31, 9 (2018), 1680–1692.
- [67] Si Zhang, Hanghang Tong, Long Jin, Yinglong Xia, and Yunsong Guo. 2021. Balancing consistency and disparity in network alignment. In *Proceedings of the 27th ACM SIGKDD conference on knowledge discovery & data mining*. 2212–2222.
- [68] Si Zhang, Hanghang Tong, Yinglong Xia, Liang Xiong, and Jiejun Xu. 2020. Nettrans: Neural cross-network transformation. In *Proceedings of the 26th ACM SIGKDD International Conference on Knowledge Discovery & Data Mining*. 986–996.
- [69] Qinghai Zhou, Liangyue Li, Xintao Wu, Nan Cao, Lei Ying, and Hanghang Tong. 2021. Attent: Active attributed network alignment. In *Proceedings of the Web Conference 2021*. 3896–3906.
- [70] Zhi-Hua Zhou. 2012. *Ensemble methods: foundations and algorithms*. CRC press.
- [71] Marinka Zitnik and Jure Leskovec. 2017. Predicting multicellular function through multi-layer tissue networks. *Bioinformatics* 33, 14 (2017), i190–i198.

## 7 APPENDIX

### 7.1 More Experiments

**7.1.1 Datasets. Douban Online-Offline** [65]. In this context, we align two social network graphs, the online graph and the offline graph. In the online graph, nodes correspond to users, and edges depict interactions between users (such as replies to messages) on the website. The offline graph is constructed based on user co-occurrence in social gatherings, with the location of a user serving as node features in both graphs. The online graph is larger and encompasses all users in the offline graph. For this dataset, 1,118 users appearing in both graphs are utilized as the ground truth.

**ACM-DBLP** [66]. The co-author networks, ACM and DBLP, are derived from publication data in four research areas. In both networks, nodes represent authors and edges signify co-author relations. Node features indicate the number of papers published in various venues. There are 6,325 common authors shared between the two networks. **Allmovie-Imdb** [47] The Allmovie network is derived from the Rotten Tomatoes website, where two films are connected by an edge if they share at least one common actor. The Imdb network is constructed from the Imdb website using a similar approach. The alignment indicates film identity, incorporating 5,174 anchor links. **Cora** and **Citeseer** [35] are two citation networks where nodes correspond to scientific publications and edges represent citation links. Each publication node in the graph is characterized by a 0/1-valued word vector, indicating the absence/presence of the corresponding word from the dictionary.

**PPI** [71] represents a protein-protein interaction network where nodes represent proteins and edges represent interactions between proteins. The node features include motif gene sets and immunological signatures.

**7.1.2 More Evaluation Metrics.** Apart from Hits@ $k$ , **mean average precision (MAP)** is employed to evaluate the accuracy of the predicted node rankings. Specifically, it is calculated as follows:

$$\text{MAP} = \frac{\sum_{(u_i, v_k) \in \mathcal{M}^*} \frac{1}{\text{Rank}(u_i, v_k)}}{|\mathcal{M}^*|}, \quad (20)$$

where  $\text{Rank}(u_i, v_k)$  denotes ranking of  $v_k$  according to  $\mathbf{T}(i, \cdot)$  by descending order.

**7.1.3 Implementation Details.** All experiments are conducted on a high-performance computing server equipped with a GV-4090-24GD GPU. We successfully replicate the results of all baselines except UHOT-GM and report their highest matching accuracy in the learning process.

For our model, the number of GNN layers (in the GRAFT and WL modules) are set to 2, the learning rate is fixed to 0.01, and the feature dimension is 32. In the EL module, we construct the bipartite graph edges by setting  $r = 5$ .

Since the maximum weight matching algorithm of the EL module returns a one-to-one matching, in Table 4, the Hits@5 and Hits@10 values of CombAlign are obtained from the model variant without EL.

**7.1.4 Evaluation of Accuracy via Mean Average Precision (MAP).** In Table 9, we present a comparative analysis of the MAP values for

various models, showcasing the efficacy of the CombAlign model. Generally speaking, the MAP results show similar qualitative conclusions as Hits@1, while CombAlign consistently achieves the best performance.

**7.1.5 Convergence Analysis.** We simultaneously visualize the prediction accuracy and the model loss (i.e., the Gromov-Wasserstein discrepancy) on three real-world datasets at different epochs, as shown in Figure 11. With the increase of epochs, the loss gradually decreases to almost approaching zero, meanwhile, the Hits@1 value gradually converges.

**7.1.6 Impact of Hyper-parameters.** In addition to the sensitivity experiments in the main paper, we also conduct experiments to evaluate the robustness of the model in terms of MAP by varying feature dimensions and the number of GNN layers. Additionally, we also evaluate the choice of  $r$  in bipartite edge construction of the EL module. As shown in Figure 10, our model performs well across different feature dimensions. However, as the number of GNN layers increases, the performance has a notable decrease on the Douban dataset. This phenomenon may be attributed to over-smoothing caused by excessive layer stacking. As for the selection of  $r$ , there is a slight improvement when its value increases from 3 to 5, followed by relatively stable performance.

### 7.2 The Proximal Point Method

Following the previous work [4, 44, 55], we employ the proximal point method [54, 55] to iteratively learn the optimal transport. Algorithm 6 gives the details of the proximal point method. Specifically, by replacing the KL-divergence in Equation 12 with an entropic regularizer  $H(\mathbf{T})$ , the problem can be solved by the Sinkhorn-Knopp algorithm [7, 38]. The  $\text{diag}(\cdot)$  function converts a  $d$ -dimensional vector to a diagonal matrix of size  $d \times d$ , while  $\odot$  and  $\dot{\div}$  represent element-wise multiplication and division, respectively.

---

#### Algorithm 6: Proximal Point Method for GW Discrepancy

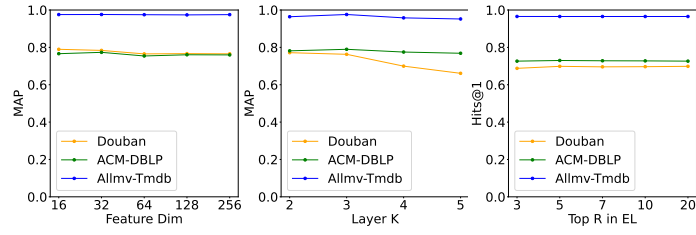
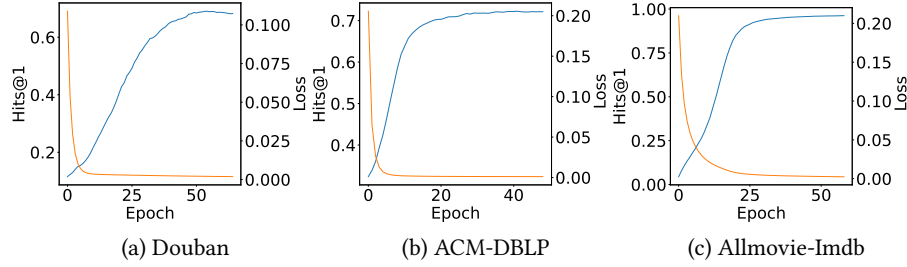
---

**Input:** Intra-graph cost matrices  $\mathbf{C}_s$  and  $\mathbf{C}_t$ , marginals  $\boldsymbol{\mu}$  and  $\boldsymbol{\nu}$ ,  $\tau_T$ , the number of inner iterations  $I_{ot}$

**Output:**  $\mathbf{T}_{GW}^{(i)}$ , the OT-based alignment probability in the  $i$ -th iteration

- 1 Initialize  $\mathbf{T}^{(0)} \leftarrow \boldsymbol{\mu} \boldsymbol{\nu}^\top$  and  $\mathbf{a} \leftarrow \boldsymbol{\mu}$ ;
- 2 **for**  $i' = 1$  to  $I_{ot}$  **do**
- 3     Calculate the  $\mathbf{C}_{gwd}$  following Equation 2;
- 4     Set  $\mathbf{G} \leftarrow \exp\left(\frac{\mathbf{C}_{gwd}}{\tau_T}\right) \odot \mathbf{T}^{(i')}$ ;  
      // Sinkhorn-Knopp algorithm
- 5     **for**  $j = 0$  to  $J$  **do**
- 6          $\mathbf{b} \leftarrow \frac{\boldsymbol{\nu}}{\mathbf{G}^\top \mathbf{a}}$ ;
- 7          $\mathbf{a} \leftarrow \frac{\boldsymbol{\mu}}{\mathbf{G} \mathbf{b}}$ ;
- 8          $\mathbf{T}^{(i'+1)} \leftarrow \text{diag}(\mathbf{a}) \mathbf{G} \text{diag}(\mathbf{b})$ ;
- 9      $\mathbf{T}_{GW}^{(i)} \leftarrow \mathbf{T}^{(I_{ot})}$ ;
- 10 **return**  $\mathbf{T}_{GW}^{(i)}$ ;

---


**Figure 10: Sensitivity analysis of CombAlign on three real-world datasets.**

**Figure 11: Convergence analysis on three real-world datasets.**
**Table 9: Comparison of model performance in terms of MAP.**

Datasets	Metrics	GAlign	WAlign	GTCAlign	GWL	SLOTAlign	UHOT-GM	CombAlign
Douban Online-Offline	Hits@1	45.26	39.45	61.79	3.29	51.43	<u>62.97</u>	<b>70.57</b>
	MAP	56.32	46.22	<u>69.77</u>	5.79	61.29	-	<b>77.08</b>
ACM-DBLP	Hits@1	<u>70.20</u>	63.43	60.92	56.36	66.04	69.53	<b>73.35</b>
	MAP	<u>77.49</u>	70.76	67.67	64.82	73.76	-	<b>79.55</b>
Allmovie-Imdb	Hits@1	82.14	52.61	84.73	87.82	<u>90.60</u>	-	<b>96.57</b>
	MAP	84.96	61.17	87.12	89.64	<u>91.61</u>	-	<b>97.31</b>
Cora	Hits@1	99.45	98.45	99.35	86.19	<u>99.48</u>	99.41	<b>99.56</b>
	MAP	99.69	99.18	99.69	89.71	<u>99.71</u>	-	<b>99.75</b>
Citeseer	Hits@1	<u>99.73</u>	97.81	99.68	57.05	99.25	-	<b>99.82</b>
	MAP	99.84	98.88	<u>99.89</u>	61.31	99.62	-	<b>99.91</b>
PPI	Hits@1	89.20	88.51	89.25	86.76	<u>89.30</u>	87.10	<b>89.70</b>
	MAP	90.72	89.02	<u>90.80</u>	87.74	90.76	-	<b>91.12</b>